Fractional Langevin equation far from equilibrium: Riemann-Liouville fractional Brownian motion, spurious nonergodicity, and aging

Qing Wei [1,*] Wei Wang [2,†] Yifa Tang [1,3,‡] Ralf Metzler [2,4,§] and Aleksei Chechkin [2,4,5,6,‖]

[1] LSEC, ICMSEC, Academy of Mathematics and Systems Science, Chinese Academy of Sciences, Beijing 100190, China

[2] University of Potsdam, Institute of Physics & Astronomy, 14476 Potsdam-Golm, Germany

[3] School of Mathematical Sciences, University of Chinese Academy of Sciences, Beijing 100049, China

[4] Asia Pacific Centre for Theoretical Physics, Pohang 37673, Republic of Korea

[5] Faculty of Pure and Applied Mathematics, Hugo Steinhaus Center, Wrocław University of Science and Technology, Wyspianskiego 27, 50-370 Wrocław, Poland

[6] German-Ukrainian Core of Excellence, Max Planck Institute of Microstructure Physics, Weinberg 2, 06120 Halle, Germany

(Received 14 August 2024; accepted 11 December 2024; published 13 January 2025)

We consider the fractional Langevin equation far from equilibrium (FLEFE) to describe stochastic dynamics which do not obey the fluctuation-dissipation theorem, unlike the conventional fractional Langevin equation (FLE). The solution of this equation is Riemann-Liouville fractional Brownian motion (RL-FBM), also known in the literature as FBM II. Spurious nonergodicity, stationarity, and aging properties of the solution are explored for all admissible values $\alpha > 1/2$ of the order α of the time-fractional Caputo derivative in the FLEFE. The increments of the process are asymptotically stationary. However when $1/2 < \alpha < 3/2$, the time-averaged mean-squared displacement (TAMSD) does not converge to the mean-squared displacement (MSD). Instead, it converges to the mean-squared increment (MSI) or structure function, leading to the phenomenon of spurious nonergodicity. When $\alpha \geqslant 3/2$, the increments of FLEFE motion are nonergodic, however the higher order increments are asymptotically ergodic. We also discuss the aging effect in the FLEFE by investigating the influence of an aging time t_a on the MSD, TAMSD and autocovariance function of the increments. We find that under strong aging conditions the process becomes ergodic, and the increments become stationary in the domain $1/2 < \alpha < 3/2$.

DOI: 10.1103/PhysRevE.111.014128

I. INTRODUCTION

In his famous note "On the Theory of Brownian Motion" of 1908, Paul Langevin formulated Newton's second law for a test Brownian particle immersed in a fluid or gas at equilibrium [1]. In modern terms, Langevin's stochastic differential equation for the position x of the particle at time t is given by (in this paper, we consider the one-dimensional case) [2–4]

$$m\frac{d^2x(t)}{dt^2} = -m\eta\frac{dx(t)}{dt} + f(t), \qquad (1)$$

where m is the mass of the particle and η is friction coefficient with dimension time^{-1}. The first term on the right-hand side represents the frictional force exerted by the medium and the second term is the random force $f(t)$ due to the random collisions of the surrounding molecules with the test particle. In the theory of Brownian motion, the random force is chosen as zero-mean white Gaussian noise with autocovariance function (ACF) $\langle f(t)f(t')\rangle = 2\mathcal{K}\delta(t-t')$, where $\mathcal{K}$ is the noise intensity and $\delta(\cdot)$ is the Dirac delta function, following $\int_{-\infty}^{\infty}\delta(\tau)d\tau = 1$. Importantly, the friction and random forces are not independent: the noise intensity and friction coefficient are related by $\mathcal{K} = k_BTm\eta$, in which k_B is the Boltzmann constant and T is the temperature of the gas or fluid in which the Brownian particle is immersed. The last relation is the simplest example of the fluctuation-dissipation theorem (FDT) for a particle in an equilibrated bath or at thermal equilibrium [5]. A noise obeying the FDT is called internal [6] and otherwise external. The overdamped form of the Langevin equation neglects the inertial term on the left hand side of Eq. (1) and is used for the description of Brownian motion in a medium with strong friction, that is, large viscosity,

$$\frac{dx(t)}{dt} = \sqrt{2K}\xi(t). \qquad (2)$$

A typical example for a Brownian particle are micron-sized colloidal spheres in water. In Eq. (2), $\xi(t)$ denotes zero-mean white Gaussian noise with $\langle\xi(t)\xi(t')\rangle = \delta(t-t')$ and K of physical dimension length^2/time is the diffusion coefficient that follows the Einstein relation or FDT $K = k_BT/(m\eta)$. Eq. (2) encodes the familiar linear time dependence of the mean-squared displacement (MSD), $\langle x^2(t)\rangle = 2Kt$, which is called normal diffusion. In what follows we will deal with generalizations of the overdamped Langevin equation (2).

Over the past decades, anomalous diffusion phenomena characterized by a nonlinear dependence of the MSD have been found ubiquitously in nature and studied intensively.

*Contact author: weiqingbambi@gmail.com
†Contact author: weiwangnuaa@gmail.com
‡Contact author: tyf@lsec.cc.ac.cn
§Contact author: rmetzler@uni-potsdam.de
‖Contact author: chechkin@uni-potsdam.de

Here we refer the reader to several monographs [7–10] as well as reviews [11–15] and numerous references therein. In the most typical form of anomalous diffusion with a power-law form $\langle x^2(t)\rangle \simeq t^\alpha$ and scaling exponent α. One distinguishes between slow diffusion, or subdiffusion if the MSD grows sublinearly in time ($0 < \alpha < 1$), and fast diffusion, or superdiffusion characterized by superlinear increase of the MSD ($\alpha > 1$). There are two generic Langevin-like models based on generalizations of Eqs. (1) and (2), which account for anomalous diffusion in a lot of practical applications.

The first generalization is related to the fractional Brownian motion (FBM), introduced by Kolmogorov [16], and Mandelbrot and van Ness [17], which can be defined via the Langevin equation

$$\frac{d}{dt}x(t) = \sqrt{2K_\alpha}\xi_\alpha(t), \tag{3}$$

where K_α is the generalized diffusion coefficient with physical dimension length^2/time$^\alpha$, and $\xi_\alpha(t)$ is the fractional Gaussian noise, that is a stationary Gaussian process with zero-mean and long-time power-law decay of the ACF ($t' \gg t$), $\langle \xi_\alpha(t)\xi_\alpha(t')\rangle \sim [\alpha(\alpha-1)/2]|t_1 - t_2|^{\alpha-2}$ for which the anomalous diffusion exponent $\alpha \in (0, 2]$. In the mathematical literature, FBM is defined with the Hurst exponent $H = \alpha/2$. The ordinary BM in Eq. (2), corresponds to the case $\alpha = 1$ [18]. The MSD of FBM grows like $\simeq t^\alpha$, so FBM accounts for both sub- and superdiffusion phenomena[1]. Importantly, the FBM (3) does not fulfill the FDT and thus cannot describe diffusion in systems close to equilibrium. Instead, the noise is considered to be external which is immanent to open systems [6], e.g., living cells [19,20], crowded fluids [21,22], movement ecology [23], serotonergic brain fibers [24,25], or financial markets [26–28].

The second model, the generalized Langevin equation (GLE) suggested by Mori and Kubo [3,5,29], provides a stochastic description of thermalized systems near equilibrium. The overdamped form reads [5,29]

$$\int_0^t \gamma(t-t')\frac{dx(t')}{dt'}dt' = \zeta(t), \tag{4}$$

in which $\gamma(t)$ is the friction kernel of dimension time^{-2} and $\zeta(t)$ is a Gaussian fluctuating driving force whose ACF is coupled to the friction kernel by the FDT $\langle\zeta(t)\zeta(t')\rangle = [k_BT/m]\gamma(|t-t'|)$. The GLE reduces to the normal Langevin equation when $\gamma(t) = 2\eta\delta(t)$ [30,31]. In the cytoplasm of a biological cell or cell extract, a particle moves through a medium characterized by macromolecular crowding and the presence of elastic elements, which provides the cytoplasm with viscoelastic properties. In other words, the cytoplasm "pushes back" and ensures long-time correlations in the particle's trajectory [19]. The particle then exhibits subdiffusive behavior, which is modeled by the fractional Langevin equation (FLE) [32] that is a particular case of the GLE in Eq. (4) with a power-law friction kernel $\gamma_\alpha(t) \propto t^{-\alpha}$, where $0 < \alpha < 1$ [33,34].

[1]Note that in order to describe subdiffusion, the integral from zero to infinity over the ACF of the noise must be zero [17].

The FLE can be conveniently written in terms of the Caputo fractional derivative of order $n-1 < \alpha < n, n \in \mathbb{N}^+$, which is defined as [35,36]

$${}_0^C D_t^\alpha[f(t)] \equiv \frac{d^\alpha x(t)}{dt^\alpha} = \int_0^t f^{(n)}(u)\frac{(t-u)^{-\alpha+n-1}}{\Gamma(n-\alpha)}du. \tag{5}$$

In particular, when $\alpha = n \in \mathbb{N}_0$, the Caputo derivative is reduced to the normal derivative ${}_0^C D_t^n[f(t)] = f^{(n)}(t)$ [37].

Then the overdamped form of the FLE reads

$$\eta_\alpha \frac{d^\alpha x(t)}{dt^\alpha} = \zeta_\alpha(t), \quad 0 < \alpha < 1, \tag{6}$$

where the noise $\zeta_\alpha(t)$ satisfies the FDT $\langle\zeta_\alpha(t)\zeta_\alpha(t')\rangle = [k_BT\eta_\alpha/(m\Gamma(1-\alpha))]|t-t'|^{-\alpha}$ with η_α of dimension time$^{\alpha-2}$. Its MSD grows like $\langle x^2(t)\rangle = 2K_\alpha t^\alpha$ with $K_\alpha = [k_BT/(\Gamma(1+\alpha)m\eta_\alpha)]$, which shows that the FLE (6) describes a subdiffusion process. According to the δ-function property $\lim_{\alpha\to 1^-}[|\tau|^{-\alpha}/\Gamma(1-\alpha)] = 2\delta(\tau)$ [38], the Markovian limit of this description is obtained with $\langle\zeta_1(t)\zeta_1(t')\rangle = 2[k_BT\eta_1/m]\delta(t-t')$, which corresponds to the overdamped Langevin equation (2).

In this paper, we consider another variant of the Langevin equation that we call fractional Langevin equation far from equilibrium (FLEFE),

$$\frac{d^\alpha x(t)}{dt^\alpha} = \sqrt{2K_\alpha}\xi(t), \tag{7}$$

in which the parameter is defined for all $\alpha > 0$, $\xi(t)$ is white Gaussian noise as defined above and the fractional derivative is to be interpreted in the Caputo sense (5). Hereafter, we show that the statistical quantities of the FLEFE exist for $\alpha > 1/2$. The three Langevin equations, i.e., the FBM (3), the FLE (6) and the FLEFE (7), constitute a set of generic Langevin models that account for memory effects, but in a different way: in the FBM case, the particle is driven by an external random force exhibiting power-law correlations; in the FLE and FLEFE cases, the memory effects arise from the viscoelastic properties of the media; the FLE obeys the FDT, but the FBM and FLEFE do not.

The FLEFE was introduced by Eab and Lim [39] who also derived the exact solution which we reproduce in Sec. IV. In particular, with zero initial conditions the solution is reduced to the Riemann-Liouville integral representation of FBM (RL-FBM) proposed by Lévy [40], which is also known as FBM II in the literature [27]. Moreover, in Ref. [41], Lim discussed ensemble averages such as the MSD and the mean-squared increment (MSI) of the RL-FBM in the domain $1/2 < \alpha < 3/2$ (which as we will see below, corresponds to the Hurst exponent regime $0 < H < 1$). Lim demonstrated that RL-FBM lacks the stationary property of the increments, unlike the standard FBM, which has stationary increments as described by Eq. (3). Instead, they identified an asymptotic stationarity of the increments in the long-time behavior of RL-FBM indicating that in this domain of the exponent α, RL-FBM is asymptotically ergodic at long times.

Here, we aim to develop the theory of FLEFE motion, Eq. (7), for all $\alpha > 1/2$ beyond the standard Hurst exponent regime $0 < H < 1$, by focusing on measurable quantities including the MSD, the time-averaged MSD (TAMSD), the MSI and the ACF (i.e., the autocovariance of the increments).

We point the attention of the reader to the nonequivalence of the generic definitions of the MSD and the mean TAMSD which leads to a surprising spurious nonergodicity [42] in the regime $1/2 < \alpha < 3/2$, and reveal a distinct coincidence between the mean TAMSD and the MSI in the long-time limit. In view of the nonstationarity of the increments of FLEFE motion, it is therefore a natural question to explore aging effects, i.e., the explicit dependence of physical observables on the time span t_a between the original system preparation and the start of the recording of the particle motion.

The paper is organized as follows. In Sec. II, we recall the fundamental concepts of diffusion processes we plan to discuss in this paper. In Sec. III, we give a reminder of the characteristic properties of two major stochastic processes, FBM and FLE motion. In Sec. IV, we discuss the results for RL-FBM, as the solution of FLEFE with zero initial condition. Specifically, we focus on ergodic and asymptotically stationary properties by using the MSD, the MSI, and the mean TAMSD for all $\alpha > 1/2$. In Sec. V, we derive the form of the $(n+1)$th order MSI, and discuss its stationary property. In Sec. VI, the aging effects for all $\alpha > 1/2$ on the MSD and mean TAMSD are considered. In Sec. VII, we summarize and discuss our results.

II. STATISTICAL CHARACTERISTICS OF DIFFUSION PROCESSES

To quantify the averaged diffusive behavior of tracer particles, the conventional measurable quantity is the MSD, defined by averaging over the ensembles of trajectories $x_i(t)$ at time t with respect to each trajectory's initial position of the diffusing particles such as

$$\langle x^2(t)\rangle = \frac{1}{N}\sum_{i=1}^{N}(x_i(t) - x_i(0))^2. \tag{8}$$

Here N is the total number of trajectories. The MSI, qualifying the increment of displacement during the lag time Δ starting at physical time t, is defined as the mean-squared of the increment in the form [43]

$$\left\langle x_\Delta^2(t)\right\rangle = \langle [x(t+\Delta) - x(t)]^2\rangle. \tag{9}$$

The MSI is equal to the MSD $\langle x^2(\Delta)\rangle$ if the process has stationary increments. The definition of the MSI is identical to the structure function originally introduced by Kolmogorov and Yaglom in their works on locally homogeneous and isotropic turbulence [44–48].

Alternatively, the diffusion of an individual particle can be quantified from a single particle trajectory $x(t)$ via the TAMSD [15,49]

$$\overline{\delta^2(\Delta)} = \frac{1}{T-\Delta}\int_0^{T-\Delta}[x(t'+\Delta) - x(t')]^2 dt', \tag{10}$$

where T is the length of the time series (measurement time) and Δ is the lag time. One can get the mean TAMSD by averaging over an ensemble of N individual trajectories in the form

$$\left\langle\overline{\delta^2(\Delta)}\right\rangle = \frac{1}{N}\sum_{i=1}^{N}\overline{\delta_i^2(\Delta)}. \tag{11}$$

The TAMSD is typical used to evaluate few but long-time series garnered in single particle tracking experiments, e.g., in biological cells, of geo-tagged larger animals, or of financial time series [49–52].

The concept of ergodicity which we will consider below relies on the MSD-to-TAMSD equivalence in the limit of long trajectories and short lag times, see Refs. [15,53], e.g.,

$$\lim_{\Delta/T\to 0}\overline{\delta^2(\Delta)} = \langle x^2(\Delta)\rangle. \tag{12}$$

A stochastic process with stationary increment, for instance, BM and FBM, is obviously ergodic according to this definition. Weakly nonergodic models of anomalous diffusion such as continuous time random walks with scale-free waiting times are easily distinguished from ergodic diffusion models by applying tests [54], for instance, the p-variation test [55] and the moving average vs ensemble average test [56]. Numerous stochastic processes reveal weak ergodicity breaking that violates the equivalence of the MSD and TAMSD. Starting with the work of Bouchaud [57], there has been growing interest in weak ergodicity breaking. A particular case is called ultraweak ergodicity breaking [57,58]: here the MSD deviates from the TAMSD only in the prefactor, albeit they have the same scaling exponent. The work by Mardoukhi *et al.* [42] reported that the Ornstein-Uhlenbeck process, known as a stationary and ergodic process, leads to spurious nonergodicity due to the failure of equivalence of the generic MSD [depending on the initial condition $x(0)$] and TAMSD in Eq. (12). The authors suggested that one should compare the MSI and the TAMSD, a suggestion that we elaborate on in this paper.

In a nonstationary setting, the origin of time can no longer be chosen arbitrarily. This raises the question of aging, that is, the explicit dependence of physical observables on the time span t_a between the original preparation of the system and the start of the recording of data. Traditionally, aging is considered as a key property of glassy systems [59]. For an aged process, in which we measure the MSD starting from the aging time t_a until time t, the aged MSD is defined in the form

$$\langle x^2(t)\rangle_a = \langle [x(t_a+t) - x(t_a)]^2\rangle, \tag{13}$$

which is similar to the MSI in Eq. (9). For a nonaged process with $t_a = 0$ the standard MSD is recovered, as it should. In the aged process, the aged MSD (13) is reduced by the amount accumulated until time t_a, at which the measurement starts.

For an aged process originally initiated at $t = 0$ and measured from t_a for the duration (measurement time) T, the aged TAMSD is defined in the form [60,61]

$$\overline{\delta_a^2(\Delta)} = \frac{1}{T-\Delta}\int_{t_a}^{T+t_a-\Delta}[x(t'+\Delta) - x(t')]^2 dt', \tag{14}$$

as a function of the lag time Δ and the aging time t_a. Averaging over an ensemble of N individual trajectories in the form

$$\left\langle\overline{\delta_a^2(\Delta)}\right\rangle = \frac{1}{N}\sum_{i=1}^{N}\overline{\delta_{a,i}^2(\Delta)} \tag{15}$$

defines the mean aged TAMSD.

III. STATISTICAL PROPERTIES OF FBM AND FLE

FBM and FLE are important processes to describe anomalous diffusion, the related quantities for these two major anomalous diffusion models are widely studied [33,62,63]. FBM and FLE have a different physical nature, albeit both models share many common features. Here we briefly recall the statistical properties of FBM and FLE.

A. FBM

The formal solution of FBM in Eq. (3) is

$$x(t)=\sqrt{2K_\alpha}\int_0^t \xi_\alpha(t')dt', \tag{16}$$

in which the anomalous diffusion exponent range is $0<\alpha\leqslant 2$.

Its ACF is [17]

$$\langle x(t_1)x(t_2)\rangle = K_\alpha\big(t_1^\alpha+t_2^\alpha-|t_2-t_1|^\alpha\big). \tag{17}$$

Using the ACF, we find that the MSD, MSI, as well as the mean TAMSD obey the same power-law [15,33]

$$\big\langle x_\Delta^2(t)\big\rangle = \langle x^2(\Delta)\rangle = \Big\langle\overline{\delta^2(\Delta)}\Big\rangle = 2K_\alpha\Delta^\alpha, \tag{18}$$

which implies that FBM is an ergodic process.

B. FLE

The solution of the overdamped FLE in Eq. (6) is given by [34]

$$x(t)=\frac{1}{\Gamma(\alpha)\eta_\alpha}\int_0^t (t-t')^{\alpha-1}\zeta_\alpha(t')dt', \tag{19}$$

in which the exponent α is defined in the range (0, 1], corresponding to normal diffusion and subdiffusion. Its ACF is [34]

$$\langle x(t_1)x(t_2)\rangle = K_\alpha\big(t_1^\alpha+t_2^\alpha-|t_2-t_1|^\alpha\big). \tag{20}$$

with the generalized diffusion coefficient $K_\alpha=k_BT/[\Gamma(1+\alpha)m\eta_\alpha]$. Thus we immediately arrive at the MSI, MSD, and mean TAMSD with the scaling behaviors [33,34]

$$\big\langle x_\Delta^2(t)\big\rangle = \langle x^2(\Delta)\rangle = \Big\langle\overline{\delta^2(\Delta)}\Big\rangle = 2K_\alpha\Delta^\alpha, \tag{21}$$

indicating that the FLE process is also ergodic.

IV. FLEFE AND RL-FBM

In what follows, we consider the FLEFE (7), in which the exponent is defined for arbitrary $\alpha>0$, and the initial conditions are given by $x^{(k)}(0)$, $k=0,\dots,[\alpha]$, where $[\cdot]$ denotes the integer part of a real-valued positive number. To emphasize the remarkable difference between the FLEFE and the FLE, we first note that in the FLEFE, the random force is represented by white Gaussian noise, breaking the FDT relation, and second, that the FLEFE motion is well defined for arbitrary exponent $\alpha>0$.

The solution of Eq. (7) was given as [39]

$$x(t)=a(t)+\sqrt{2K_\alpha}\int_0^t\frac{(t-t')^{\alpha-1}}{\Gamma(\alpha)}\xi(t')dt', \tag{22}$$

in which the first part solely depends on the initial conditions, $a(t)=\sum_{k=0}^{[\alpha]}t^kx^{(k)}(0)/\Gamma(k+1)$, and the second part is identical to Lévy's formulation of FBM (RL-FBM) with Hurst exponent $H=\alpha-1/2$ [17].

Without loss of generality, we here introduce the new process $x(t)\equiv x(t)-\langle x(t)\rangle$, such that $\langle x(t)\rangle=0$. Equivalently, if one assumes that all initial conditions are zero, i.e., $a(t)=0$, the solution of the FLEFE (22) is equivalent to the RL-FBM [41]

$$x(t)=\sqrt{2K_\alpha}\int_0^t\frac{(t-t')^{\alpha-1}}{\Gamma(\alpha)}\xi(t')dt'. \tag{23}$$

RL-FBM was first introduced by Lévy [40] and defined in terms of a Riemann-Liouville fractional integral with initial condition at $t=0$. In contrast to the equilibrated FBM developed by Mandelbrot and van Ness, Lévy's RL-FBM is a stochastic process with nonstationary increments. This point gives rise to interesting differences between FBM and FLEFE, as we now explore.

A. MSD

The ACF of FLEFE motion is given by (supposing that $t_1\geqslant t_2$)

$$\langle x(t_1)x(t_2)\rangle = \frac{2K_\alpha t_2^\alpha t_1^{\alpha-1}}{\alpha\Gamma(\alpha)^2}\times {}_2F_1\left(1-\alpha,1;\alpha+1;\frac{t_2}{t_1}\right), \tag{24}$$

where

$${}_2F_1(a,b;c;z)=\frac{\Gamma(c)}{\Gamma(b)\Gamma(c-b)}\int_0^1\frac{t^{b-1}(1-t)^{c-b-1}}{(1-tz)^a}dt \tag{25}$$

is the hypergeometric function. By taking $t_1=t_2=t$ in the two-point correlation function (24) and using the formula [64]

$${}_2F_1(a,b;c;1)=\frac{\Gamma(c)\Gamma(c-a-b)}{\Gamma(c-a)\Gamma(c-b)},\quad \mathbb{R}(c)>\mathbb{R}(a+b), \tag{26}$$

one can obtain the MSD [39]

$$\langle x^2(t)\rangle = \frac{2K_\alpha}{(2\alpha-1)\Gamma(\alpha)^2}t^{2\alpha-1}, \tag{27}$$

and thus one can see that the MSD is meaningful for all $\alpha>1/2$. It is worth noting that this requirement for the exponent α in the FLEFE differs from, e.g., those in SBM and FBM [65].

B. MSI

Lim derived the MSI of RL-FBM in the form [41]

$$\begin{aligned}\big\langle x_\Delta^2(t)\big\rangle &= \langle[x(t+\Delta)-x(t)]^2\rangle\\ &=\frac{2K_\alpha}{\Gamma(\alpha)^2}\Delta^{2\alpha-1}\left\{L_\alpha\left(\frac{t}{\Delta}\right)+\frac{1}{2\alpha-1}\right\},\end{aligned} \tag{28}$$

where the integral $L_\alpha(z)$ is given by

$$L_\alpha(z)=\int_0^z[(1+s)^{\alpha-1}-s^{\alpha-1}]^2ds. \tag{29}$$

In explicit form, the MSI of RL-FBM can be expressed via the hypergeometric function [64] or the H-function [66] [see the derivation of Eq. (A4) in Appendix A]

$$\left\langle x_\Delta^2(t)\right\rangle = \frac{2K_\alpha}{(2\alpha-1)\Gamma(\alpha)^2}[(t+\Delta)^{2\alpha-1}+t^{2\alpha-1}] - \frac{4K_\alpha t^\alpha (t+\Delta)^{\alpha-1}}{\alpha\Gamma(\alpha)^2}\,{}_2F_1\left(1-\alpha,1;1+\alpha;\frac{t}{t+\Delta}\right). \quad (30)$$

We note here that both expressions (28) and (30) of the MSI are valid for all $\alpha > 1/2$ and underline the nonstationary nature of RL-FBM. In particular, when α approaches 1, the hypergeometric function ${}_2F_1(1-\alpha, 1; 1+\alpha; t/(t+\Delta)) = 1$ and thus $\langle x_\Delta^2(t)\rangle = 2K_1\Delta$.

For sufficiently short times $t \ll \Delta$, the integral $L_\alpha(t/\Delta) \approx 0$ in Eq. (28), and the MSI reads

$$\left\langle x_\Delta^2(t)\right\rangle \sim \frac{2K_\alpha}{(2\alpha-1)\Gamma(\alpha)^2}\Delta^{2\alpha-1}, \quad (31)$$

which is identical to the MSD (27) of RL-FBM.

We proceed to discuss the MSI in the long-time limit $t \gg \Delta$ in the three relevant different regimes for the order α of the fractional derivative in the FLEFE (RL-FBM). We arrive at the same approximation for the MSI by using two approaches: The first one, which is presented in the main text, uses the approximation of the integral Eq. (28), while the second, one applies a series expansion of the hypergeometric function or the H-function in Eq. (30); the latter is shown in Appendix A.

1. Case $1/2 < \alpha < 3/2$

In the long-time limit $t \gg \Delta$, the integral in Eq. (28) converges as [67]

$$L_\alpha\left(\frac{t}{\Delta}\right) + \frac{1}{2\alpha-1} \approx \int_0^\infty [(1+s)^{\alpha-1} - s^{\alpha-1}]^2 ds + \frac{1}{2\alpha-1} = \frac{\Gamma(\alpha)^2}{\Gamma(2\alpha)|\cos(\pi\alpha)|}, \quad (32)$$

and thus we arrive at the stationary MSI approximated as [41]

$$\left\langle x_\Delta^2(t)\right\rangle \sim \frac{2K_\alpha}{\Gamma(2\alpha)|\cos(\pi\alpha)|}\Delta^{2\alpha-1}, \quad (33)$$

which depends solely on the lag time Δ. The MSI becomes stationary in the long-time regime $t \gg \Delta$ and has the same anomalous diffusion exponent as the MSD (27) of RL-FBM, but deviates from the MSD by a constant prefactor.

2. Case $\alpha > 3/2$

For $\alpha > 3/2$, the integral in Eq. (28) asymptotically reads

$$L_\alpha\left(\frac{t}{\Delta}\right) = \int_0^{t/\Delta} s^{2\alpha-2}[(1+s^{-1})^{\alpha-1} - 1]^2 ds \sim \frac{(\alpha-1)^2}{2\alpha-3}\left(\frac{t}{\Delta}\right)^{2\alpha-3}, \quad (34)$$

and thus the MSI is given by

$$\left\langle x_\Delta^2(t)\right\rangle \sim \frac{2(\alpha-1)^2 K_\alpha}{(2\alpha-3)\Gamma(\alpha)^2} t^{2\alpha-3}\Delta^2. \quad (35)$$

In this range of α in the FLEFE, the MSI depends ballistically on the lag time Δ and keeps a dependence on the measured time, scaling as $t^{2\alpha-3}$.

3. Case $\alpha = 3/2$

Apparently, it follows from Eqs. (33) and (35) that the case $\alpha = 3/2$ needs to be discussed separately. In this case, the MSI (9) can be rewritten as

$$\left\langle x_\Delta^2(t)\right\rangle = \frac{8K_{3/2}}{\pi}\left[L_{3/2}\left(\frac{t}{\Delta}\right) + \frac{1}{2}\right]\Delta^2, \quad (36)$$

where the integral $L_{3/2}(z)$ can be evaluated explicitly as

$$L_{3/2}(z) = \int_0^z (\sqrt{1+s} - \sqrt{s})^2 ds = z^2 + z + \frac{1}{2}[\sinh^{-1}(\sqrt{z}) - \sqrt{z}\sqrt{z+1}(2z+1)]. \quad (37)$$

When $t \gg \Delta$, the integral can be approximated by the leading term

$$L_{3/2}\left(\frac{t}{\Delta}\right) \sim \frac{1}{4}\ln\left(\frac{t}{\Delta}\right). \quad (38)$$

Therefore, inserting Eq. (38) into the Eq. (36) yields the MSI with the dominant term

$$\left\langle x_\Delta^2(t)\right\rangle \sim \frac{2K_{3/2}}{\pi}\Delta^2 \ln\left(\frac{t}{\Delta}\right), \quad (39)$$

which also implies nonstationarity in the sense that the t-dependence remains.

The MSI of RL-FBM in the long-time limit $t \gg \Delta$ for all $\alpha > 1/2$ can thus be summarized as

$$\left\langle x_\Delta^2(t)\right\rangle \sim \begin{cases} \frac{2K_\alpha}{\Gamma(2\alpha)|\cos(\pi\alpha)|}\Delta^{2\alpha-1}, & 1/2 < \alpha < 3/2 \\ \frac{2K_{3/2}}{\pi}\Delta^2\ln\left(\frac{t}{\Delta}\right), & \alpha = 3/2 \\ \frac{2(\alpha-1)^2K_\alpha}{(2\alpha-3)\Gamma(\alpha)^2}t^{2\alpha-3}\Delta^2, & \alpha > 3/2 \end{cases}. \quad (40)$$

As mentioned above, another approach to calculate the MSI is presented in Appendix A.

Unlike the FBM (3), which has stationary increments, the RL-FBM has nonstationary increments depending on the measured time t, see the explicit form of the MSI (30) of RL-FBM. In addition, we observe that the MSI tends to become approximately stationary at long times when $1/2 < \alpha < 3/2$, whereas for $\alpha \geqslant 3/2$ the MSI remains nonstationary.

C. TAMSD

According to the definition (10) of the TAMSD, the mean TAMSD of RL-FBM can be derived as (see Appendix B)

$$\left\langle\overline{\delta^2(\Delta)}\right\rangle = \frac{1}{T-\Delta}\int_0^{T-\Delta}\langle[x(t+\Delta)-x(t)]^2\rangle dt = \frac{K_\alpha}{\alpha(2\alpha-1)\Gamma(\alpha)^2}\frac{T^{2\alpha}-\Delta^{2\alpha}}{T-\Delta} + \frac{K_\alpha}{\alpha(2\alpha-1)\Gamma(\alpha)^2} \times (T-\Delta)^{2\alpha-1} - I_\alpha(\Delta,T), \quad (41)$$

where

$$I_\alpha(\Delta,T) = \frac{4K_\alpha}{\alpha\Gamma(\alpha)^2}\frac{1}{T-\Delta}\int_0^{T-\Delta}(t+\Delta)^{\alpha-1} \times t^\alpha \times {}_2F_1\left(1-\alpha,1;1+\alpha;\frac{t}{t+\Delta}\right)dt. \quad (42)$$

In what follows, we discuss the approximations of the mean TAMSD at long times, $T \gg \Delta$, in the different regimes of α.

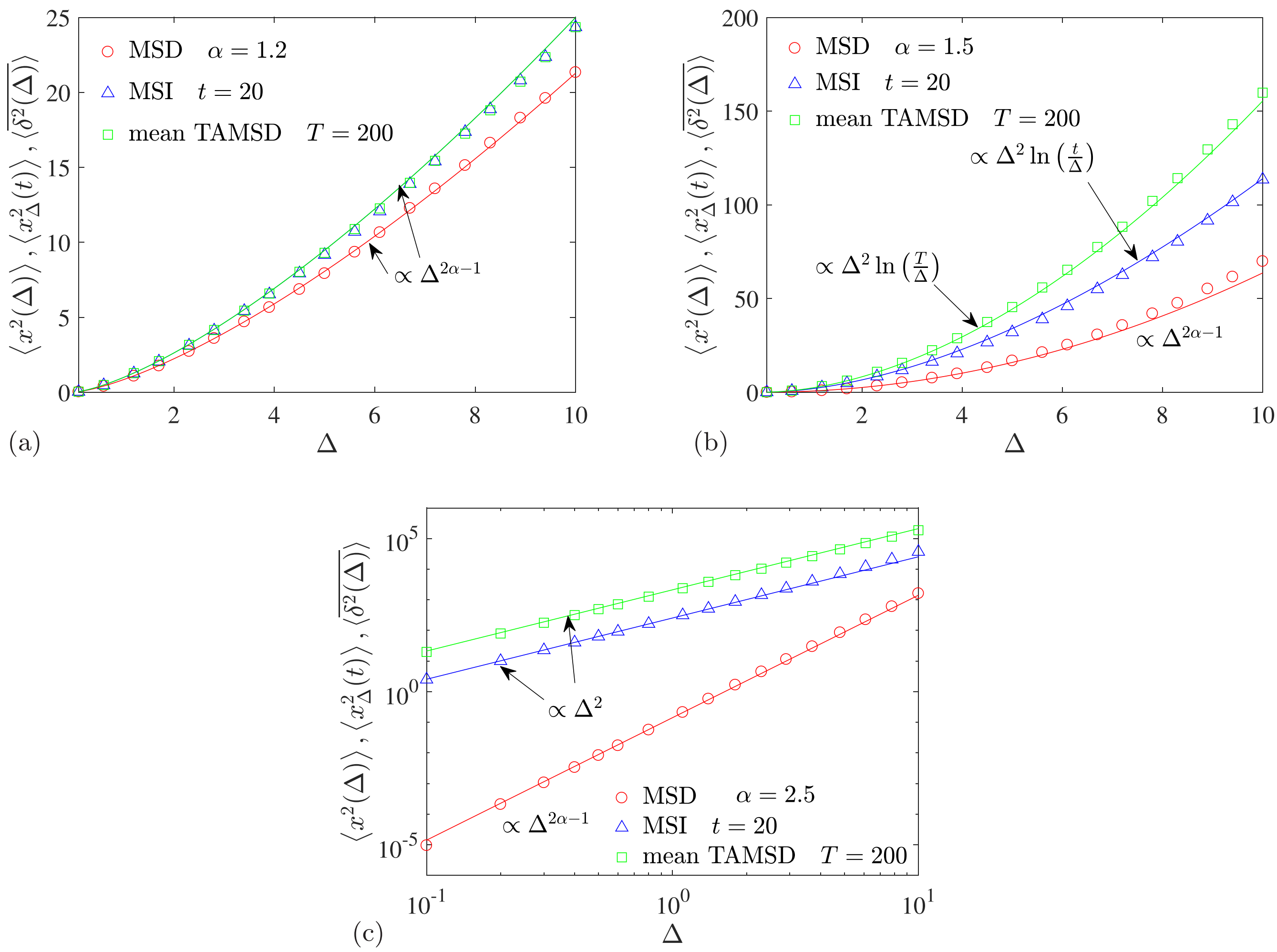

FIG. 1. Simulations (symbols) and analytical solutions (solid curves) for the MSD (27), MSI (28), and mean TAMSD (41) of RL-FBM for (a) $1/2 < \alpha < 3/2$, (b) $\alpha = 3/2$, and (c) $\alpha > 3/2$. When $1/2 < \alpha < 3/2$, the mean TAMSD is identical to the MSI and not to the MSD, leading to a spurious nonergodicity. When $\alpha \geqslant 3/2$, RL-FBM is nonergodic, and the mean TAMSD exhibits ballistic motion. Other parameters: time step $dt = 0.1$ and $K_\alpha = 0.5$. The algorithm for the simulations is presented in Appendix C.

1. Case $1/2 < \alpha < 3/2$

From the derivation of Eq. (B12) in Appendix B, we obtain the mean TAMSD of RL-FBM in Eq. (41) in the long-time limit $T \gg \Delta$ in the form

$$\left\langle\overline{\delta^2(\Delta)}\right\rangle \sim \frac{2K_\alpha}{\Gamma(2\alpha)|\cos(\pi\alpha)|}\Delta^{2\alpha-1}. \tag{43}$$

The mean TAMSD in this range of α deviates from the MSD (27) in the prefactor but has the same form as the MSI (33).

2. Case $\alpha > 3/2$

According to the derivation of Eq. (B13) in Appendix B, we obtain the mean TAMSD (41) of RL-FBM in the long-time limit $T \gg \Delta$ as

$$\left\langle\overline{\delta^2(\Delta)}\right\rangle \sim \frac{(\alpha-1)K_\alpha}{(2\alpha-3)\Gamma(\alpha)^2}T^{2\alpha-3}\Delta^2. \tag{44}$$

In this case, the mean TAMSD depends ballistically on the lag time Δ and keeps a dependence on the measurement time T with the scaling $T^{2\alpha-3}$.

3. Case $\alpha = 3/2$

Using the explicit power-logarithmic expansion of the H-function for $\alpha = 3/2$ as shown in Eq. (B14), one can obtain the approximation of the TAMSD [see the derivation of Eq. (B17) in Appendix B for details] when $T/\Delta \gg 1$,

$$\left\langle\overline{\delta^2(\Delta)}\right\rangle \sim \frac{2K_{3/2}}{\pi}\Delta^2 \ln\left(\frac{T}{\Delta}\right). \tag{45}$$

In summary, the mean TAMSD of the RL-FBM in the three relevant regimes of α reads

$$\left\langle\overline{\delta^2(\Delta)}\right\rangle \sim \begin{cases} \frac{2K_\alpha}{\Gamma(2\alpha)|\cos(\pi\alpha)|}\Delta^{2\alpha-1}, & 1/2 < \alpha < 3/2 \\ \frac{2K_{3/2}}{\pi}\Delta^2 \ln\left(\frac{T}{\Delta}\right), & \alpha = 3/2 \\ \frac{(\alpha-1)K_\alpha}{(2\alpha-3)\Gamma(\alpha)^2}\Delta^2 T^{2\alpha-3}, & \alpha > 3/2 \end{cases}. \tag{46}$$

The results of our simulations for the moments (MSD, MSI, TAMSD) are shown in Fig. 1 for RL-FBM with different α along with the analytical solutions (27) for the MSD, the MSI (28), and the mean TAMSD (41). The mean TAMSD is identical to the MSI when $1/2 < \alpha < 3/2$ for sufficiently long trajectories, while the discrepancies between the mean

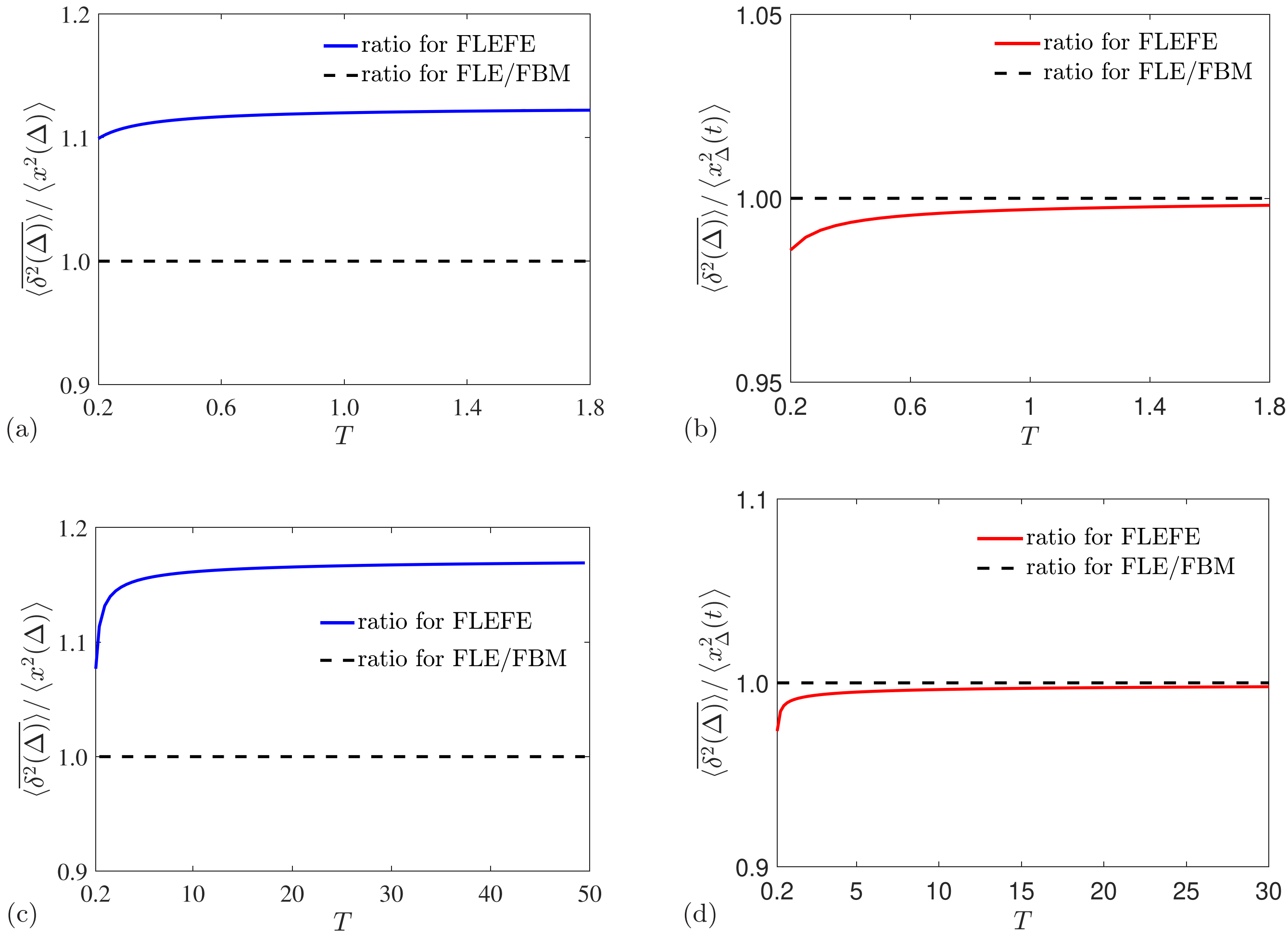

FIG. 2. Ratio $\langle\overline{\delta^2(\Delta)}\rangle/\langle x_\Delta^2(t)\rangle$ and $\langle\overline{\delta^2(\Delta)}\rangle/\langle x^2(\Delta)\rangle$ as a function of the measurement time T for different regimes. In (a) and (b), $\alpha_1 = 0.8$, and in (c) and (d), $\alpha_2 = 1.2$. When $1/2 < \alpha < 3/2$, in the long-time limit $T/\Delta \gg 1$ the mean TAMSD of RL-FBM (FLEFE) does not converge to its MSD but to the MSI in the strong aging limit. Here we set $t = T/2$ for the MIS. In all panels we chose the lag time as $\Delta = 0.1$; the time step is $dt = 0.1$, and $K_\alpha = 0.5$.

TAMSD and the MSI or MSD is retained when $\alpha \geqslant 3/2$. The algorithm of the numerical approach to generate the trajectories of RL-FBM (23) is presented in Appendix C.

Figure 2 shows the ratios of the mean TAMSD (41) to the MSD (27) and the MSI (28) with $1/2 < \alpha < 3/2$, illustrating that at long times $T/\Delta \gg 1$ the TAMSD of RL-FBM converges to the MSI rather than the MSD.

In the context of single particle tracking experiments the conclusion about ergodicity of the process (in the mean squared sense) is deduced from the convergence of the mean TAMSD to the MSD for sufficiently long trajectories, see Eq. (12) in Ref. [15]. However, by its construction, we show here that it is advisable to compare the mean TAMSD (11) with the MSI (9), rather. The MSD and MSI coincide for processes with stationary increments, such as FBM and FLE motion. However, this is not the case for processes with nonstationary increments. Taking RL-FBM as an exemplary process one can see that the mean TAMSD (46) and MSD (27) differ in the entire domain $\alpha > 1/2$ even in the long trajectory limit. This may lead to the conclusion about nonergodicity of RL-FBM in the entire domain of the fractional exponent. However, it is a spurious nonergodicity in the domain $1/2 < \alpha < 3/2$. Indeed, the increments of RL-FBM in this regime become asymptotically stationary as follows from Eq. (33), and the mean TAMSD converges to the MSI in the limit of long trajectories, compare Eqs. (33) and (43).

V. STATIONARITY OF THE $(n+1)$th ORDER MSI FOR RL-FBM

In the previous section, the MSI (40) of RL-FBM was found to be stationary at long times $t \gg \Delta$ in the regime $1/2 < \alpha < 3/2$, whereas it is nonstationary when $\alpha \geqslant 3/2$. A natural question is whether stationarity is recovered in higher orders of the MSI of RL-FBM. The aim of this section is to investigate the regime of the exponent α in which the nth order MSI will restore the stationarity property. The $(n+1)$th order increment is defined as the difference of the nth order increment over a lag time τ_{n+1} [68],

$$\Delta^{(n+1)}x(t;\tau_1,\dots,\tau_{n+1}) = \Delta^{(n)}x(t+\tau_{n+1};\tau_1,\dots,\tau_n) - \Delta^{(n)}x(t;\tau_1,\dots,\tau_n), \tag{47}$$

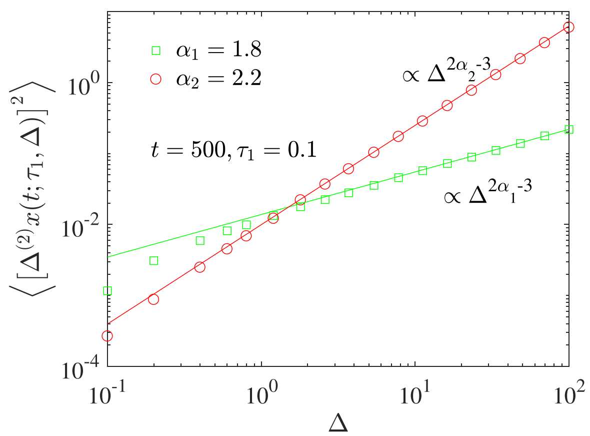

FIG. 3. Simulations (symbols) for the second order MSI of RL-FBM at long times $t \gg \Delta + \tau_1$ for different α. The theoretical result (52) is represented by solid lines. Other parameters: $dt = 0.1$, $\tau_1 = 0.1$, and $K_\alpha = 0.5$.

similar in spirit to the theory of nth order increments by Yaglom [46,47].

According to this definition, the first and second order increments are given by

$$\Delta^{(1)}x(t;\tau_1) = x(t+\tau_1) - x(t) \tag{48}$$

and

$$\Delta^{(2)}x(t;\tau_1,\tau_2) = \Delta^{(1)}x(t+\tau_2;\tau_1) - \Delta^{(1)}x(t;\tau_1), \tag{49}$$

where $\Delta^{(1)}x(t;\tau_1)$ is the first order increment of the displacement and $\Delta^{(2)}x(t;\tau_1,\tau_2)$ is an increment of the first order increment. With the approximation

$$\frac{\Delta^{(1)}x(t;\tau_1)}{\tau_1} = \frac{x(t+\tau_1)-x(t)}{\tau_1} \approx \frac{dx(t)}{dt} \tag{50}$$

at long times $t \gg \tau_1$ for the first order increment, one yields the integral representation

$$\Delta^{(1)}x(t;\tau_1) = \tau_1\frac{dx(t)}{dt} = \frac{\sqrt{2K_\alpha}}{\Gamma(\alpha-1)}\tau_1\int_0^t (t-t')^{\alpha-2}\xi(t')dt'. \tag{51}$$

We note that the integral representation of the first order increment is analogous to that of the FLEFE (22) whose MSI was found to become stationary in the regime $1/2 < \alpha < 3/2$ given by Eq. (33). Then, by a similar computation, we obtain that the second order MSI in the regime $3/2 < \alpha < 5/2$ takes on the form

$$\langle[\Delta^{(2)}x(t;\tau_1,\Delta)]^2\rangle = \langle[\Delta^{(1)}x(t+\Delta;\tau_1) - \Delta^{(1)}x(t;\tau_1)]^2\rangle \sim \frac{2K_\alpha\tau_1^2}{\Gamma(2\alpha-2)\cos(\pi\alpha)}\Delta^{2\alpha-3} \tag{52}$$

in the long-time limit $t \gg \tau_1 + \Delta$. This latter result is independent of the measurement time t, and thus revels the stationarity of the second order increment. The simulations of the second order MSI is shown in Fig. 3, showing perfect agreement with the analytical results.

More generally, the $(n+1)$th MSI

$$\begin{aligned}&\langle[\Delta^{(n+1)}x(t;\tau_1,\ldots,\tau_n,\Delta)]^2\rangle\\ &= \langle[\Delta^{(n)}x(t+\Delta;\tau_1,\ldots,\tau_n) - \Delta^{(n)}x(t;\tau_1,\ldots,\tau_n)]^2\rangle\\ &\sim \frac{2K_\alpha(\tau_1\times\ldots\times\tau_n)^2}{\Gamma(2\alpha-2n)|\cos(\pi(\alpha-n))|}\Delta^{2\alpha-2n-1}\end{aligned} \tag{53}$$

restores stationarity in the regime $(2n+1)/2 < \alpha < (2n+3)/2$.

VI. AGING EFFECTS

A distinct effect that can be probed for experimental data is aging, leading to a possible dependence on the aging time t_a. We here analyze aging for the MSD and TAMSD.

A. Aging of the MSD

As the aged MSD with aging time t_a defined in Eq. (13) is analogous to the MSI (28) of RL-FBM with process time t, one can immediately obtain the aged MSD. According to the results for the MSI of RL-FBM in Eqs. (31) and (40), we find the aged MSD for weak aging ($t_a \ll t$),

$$\langle x^2(t)\rangle_a \sim \frac{2K_\alpha}{(2\alpha-1)\Gamma(\alpha)^2}t^{2\alpha-1} \tag{54}$$

for all $\alpha > 1/2$, which is identical to the nonaged MSD (27) of RL-FBM.

For strong aging, $t_a \gg t$, the aged MSD for $1/2 < \alpha < 3/2$ is independent of the aging time t_a, exhibiting the same power-law scaling as the weakly aged MSD but with a different prefactor, whereas for $\alpha \geqslant 3/2$, the aged MSD has a ballistic scaling with the aging time t_a. We summarize the aged MSD as

$$\langle x^2(t)\rangle_a \sim \begin{cases} \frac{2K_\alpha}{\Gamma(2\alpha)|\cos(\pi\alpha)|}t^{2\alpha-1}, & 1/2 < \alpha < 3/2\\ \frac{2K_{3/2}}{\pi}t^2\ln\left(\frac{t_a}{t}\right), & \alpha = 3/2\\ \frac{2(\alpha-1)^2K_\alpha}{(2\alpha-3)\Gamma(\alpha)^2}t_a^{2\alpha-3}t^2, & \alpha > 3/2\end{cases}. \tag{55}$$

B. Aging of the TAMSD

According to the definition (14) of the aged TAMSD, we obtain the explicit aged mean TAMSD as

$$\begin{aligned}\left\langle\overline{\delta_a^2(\Delta)}\right\rangle &= \frac{1}{T-\Delta}\int_{t_a}^{T+t_a-\Delta}\langle[x(t'+\Delta)-x(t')]^2\rangle dt'\\ &= \frac{K_\alpha}{\alpha(2\alpha-1)\Gamma(\alpha)^2}\frac{(T+t_a)^{2\alpha}-(t_a+\Delta)^{2\alpha}}{T-\Delta}\\ &+ \frac{K_\alpha}{\alpha(2\alpha-1)\Gamma(\alpha)^2}\frac{(T+t_a-\Delta)^{2\alpha}-t_a^{2\alpha}}{T-\Delta}\\ &+ Q_\alpha(\Delta,t_a,T).\end{aligned} \tag{56}$$

Here $Q_\alpha(\Delta,t_a,T)$ is given via the hypergeometric function in the form

$$Q_\alpha(\Delta,t_a,T) = -\frac{4K_\alpha}{\alpha\Gamma(\alpha)^2}\frac{1}{T-\Delta}\int_{t_a}^{T+t_a-\Delta}(t+\Delta)^{\alpha-1}t^\alpha \times {}_2F_1\left(1-\alpha,1;1+\alpha;\frac{t}{t+\Delta}\right)dt. \tag{57}$$

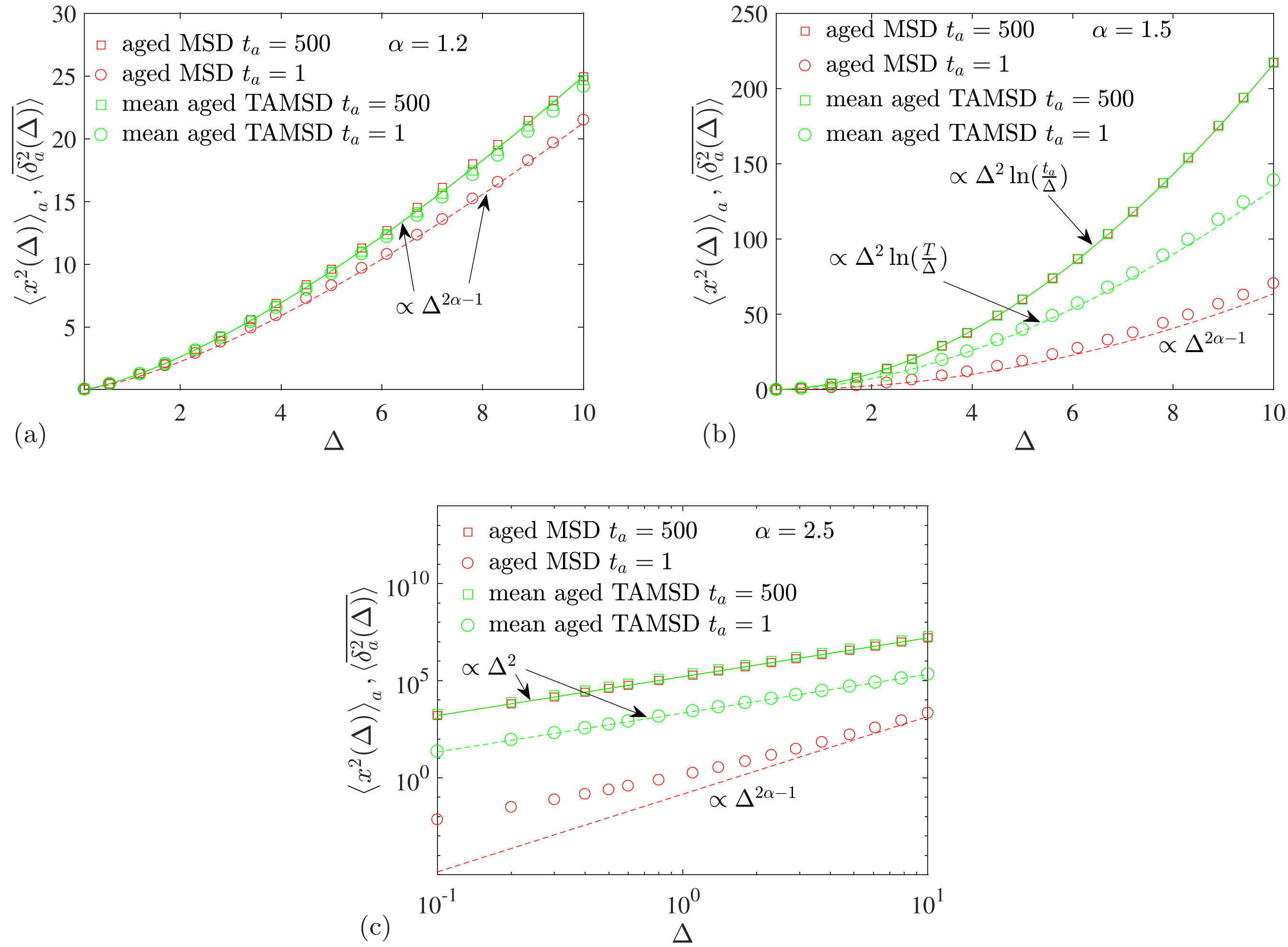

FIG. 4. Simulations and analytical results for the aged MSD and mean aged TAMSD of RL-FBM for (a) $1/2 < \alpha < 3/2$, (b) $\alpha = 3/2$, and (c) $\alpha > 3/2$. The theoretical weakly aged MSD (54), and the mean aged TAMSD (58) are represented by dashed curves, while the strongly aged MSD (55) and mean aged TAMSD (59) are represented by solid curves. Note that the (red and green) solid curves overlap since ergodicity is restored in the strong aging case. Other parameters: the simulation time step is $dt = 0.1$, the measurement time is $T = 100$ and $K_\alpha = 0.5$.

One may yield approximations of the mean aged TAMSD from expansion of the hypergeometric function or the H-function, analogous to the nonaged mean TAMSD in Appendix B. Here we simply present the results for the mean aged TAMSD of RL-FBM with different α.

Thus, for weak aging $t_a \ll T$ and $T \gg \Delta$, the results for the asymptotic behaviors are summarized as

$$\left\langle\overline{\delta_a^2(\Delta)}\right\rangle \sim \begin{cases} \frac{2K_\alpha}{\Gamma(2\alpha)|\cos(\pi\alpha)|}\Delta^{2\alpha-1}, & 1/2 < \alpha < 3/2 \\ \frac{2K_{3/2}}{\pi}\Delta^2 \ln\left(\frac{T}{\Delta}\right), & \alpha = 3/2 \\ \frac{(\alpha-1)K_\alpha}{(2\alpha-3)\Gamma(\alpha)^2}\Delta^2 T^{2\alpha-3}, & \alpha > 3/2 \end{cases}, \quad (58)$$

which coincides with the nonaged mean TAMSD (46).

For strong aging $t_a \gg T$, the mean aged TAMSD has the same asymptotics as the aged MSD (55) in the strong aging regime $t_a \gg t$, namely,

$$\left\langle\overline{\delta_a^2(\Delta)}\right\rangle \sim \begin{cases} \frac{2K_\alpha}{\Gamma(2\alpha)|\cos(\pi\alpha)|}\Delta^{2\alpha-1}, & 1/2 < \alpha < 3/2 \\ \frac{2K_{3/2}}{\pi}\Delta^2 \ln\left(\frac{t_a}{\Delta}\right), & \alpha = 3/2 \\ \frac{2(\alpha-1)^2K_\alpha}{(2\alpha-3)\Gamma(\alpha)^2}\Delta^2 t_a^{2\alpha-3}, & \alpha > 3/2 \end{cases}, \quad (59)$$

from which ergodicity is restored in the regime $1/2 < \alpha < 3/2$, since in the limit $t_a \gg T$ the collection of the increments $x(t+\Delta) - x(t)$ for $t \in [t_a, t_a + T - \Delta]$ in the TAMSD (14) changes only marginally and is almost identical to $x(t_a + \Delta) - x(t_a)$.

Simulations of the aged MSD and the mean aged TAMSD for RL-FBM with different α are shown in Fig. 4, demonstrating perfect agreement with our theoretical results in the weak and strong aging regimes. For completeness, we also analyzed the aged ACF of RL-FBM increments, and the results are presented in Appendix D.

VII. CONCLUSIONS

We introduced and discussed FLEFE motion, that provides a Langevin equation based formulation as an alternative to the FBM and FLE approaches for systems characterized by long-ranged temporal correlations. The characteristic features of FLEFE motion is its validity beyond the (standard) Hurst exponent domain $0 < H \leqslant 1$ and the ability to explore properties of nonequilibrium systems—with long-ranged correlations—that do not obey the FDT. The solution of the FLEFE with a fractional derivative of order $\alpha > 1/2$ and zero initial conditions is given by the RL-FBM (FBM II) process with Hurst exponent $H = \alpha - 1/2$. The increments or the MSI of RL-FBM become stationary (t-independent) in the domain $1/2 < \alpha < 3/2$ in the long-time limit; however, they remain nonstationary when $\alpha \geqslant 3/2$. We also showed that the $(n+1)$th MSI restores stationarity for $(2n+1)/2 < \alpha < (2n+3)/2$ in the long-time limit. The nonequivalence of the TAMSD and MSD is observed in the whole regime $\alpha > 1/2$, leading to spurious nonergodicity in the long-time limit when $1/2 < \alpha < 3/2$. More specifically, the mean TAMSD of RL-FBM converges to the MSI rather than to the MSD. We also investigated the influence of the aging time t_a on the MSD, TAMSD, and ACF of the increments. In the limit of strong aging, we demonstrated that ergodicity is restored, i.e., the disparity between aged MSD and aged mean TAMSD vanish. Under strong aging, the increment-ACF becomes stationary and solely depends on the lag time Δ in the regime $1/2 < \alpha < 3/2$, while it depends on the aging time t_a when $\alpha \geqslant 3/2$. This contrasts standard FBM and FLE which are both ergodic processes and always independent of t_a. We thus promote the MSI and the $(n+1)$th order MSI for data analysis, e.g., in terms of statistical observables [15,21,49,69,70], machine learning [71–77], or Bayesian analyses [78,79].

In nonequilibrium bio-systems, as well as other complex systems, the FLEFE may indeed be a more suitable candidate for evaluating the observed stochastic dynamics than the FBM and FLE approaches. Generally speaking, FLEFE motion will be relevant when we have nonequilibrium initial conditions, when the measurement is started immediately after inserting tracer particles such as colloidal beads or quantum dots into the medium, without waiting that they equilibrate with the medium [80]. One might also test nonequilibrium effects by deliberately moving tracer particles out of equilibrium, e.g., by puilling on them with optical tweezers [81]. Furthermore, the movement of birds, animals, or bacteria is always in nonequilibrium, such that the use of the FLEFE model appears preferable. This also holds true for inherently nonequilibrium processes such as financial market fluctuations or climate dynamics. We also note that RL-FBM (the solution of the FLEFE) can be easily modified by allowing the exponent to vary over time or space, as it is defined from a nonequilibrated initial condition at $t = 0$. In contrast, the FBM defined by Mandelbrot is less adaptable due to its definition in an equilibrated state starting from $t = -\infty$ [17]. Moreover, recent single-particle-tracking experiments revealed that intracellular transport of tracers of various sizes in cells is often not only anomalous, but also heterogeneous in time and space [82–87]. This implies that a single diffusion exponent and diffusing coefficient are insufficient to describe the underlying physical phenomena. In this sense, it is of interest to consider the FLEFE motion when both diffusivity and diffusion exponent are functions of time [88,89] or space or even randomly chosen from certain distribution [67]. In fact, RL-FBM with time-dependent exponents has been successfully validated in terms of the MSD and the power spectral density through recent experimental measurements of quantum dot motion within the cytoplasm of live mammalian cells, as observed by single-particle tracking [90]. We hope that our development of the RL-FBM model, especially in the context ergodicity, will offer experimentalists new insights into understanding the role of heterogeneity in anomalous diffusion transport phenomena.

One more relevant application of the FLEFE model may be in the physics of climate. The stochastic Markovian energy balance models (EBM) introduced by Hasselmann [91] and recognized by the award of the 2021 Nobel Prize for Physics, has achieved a great success in climate modeling. Due to the complex intake and dissipation of energy when the FDT may be broken, and taking memory effects of the global temperature anomaly into account, the FLEFE and its generalizations may be more adequate tools to describe the climate dynamics in the long-time limit, see e.g., the recent review [92] and references therein.

In the future, other potential issues for the FLEFE process are to be considered, including harmonic potential, reflecting or absorbing boundaries, resetting search [93] and delay effects [94].

ACKNOWLEDGMENTS

We acknowledge support from the German Science Foundation (DFG grant ME 1535/16-1), NSF-BMBF CRCNS (Grant No. 2112862/STAXS), and the National Natural Science Foundation of China (Grant No. 12171466). A.V.C. acknowledges BMBF Project PLASMA-SPIN Energy (Grant No. 01DK24006).

APPENDIX A: MSI

Considering the MSI given by Eq. (9) we find

$$\begin{aligned}\left\langle x_\Delta^2(t)\right\rangle &= \langle [x(t+\Delta) - x(t)]^2\rangle \\ &= \frac{2K_\alpha t^{2\alpha-1}}{(2\alpha-1)\Gamma(\alpha)^2}\left[\left(1+\frac{\Delta}{t}\right)^{2\alpha-1}+1\right] \\ &\quad - \frac{4K_\alpha t^\alpha (t+\Delta)^{\alpha-1}}{\alpha\Gamma(\alpha)^2}\times {}_2F_1\left(1-\alpha, 1; 1+\alpha; \frac{t}{t+\Delta}\right).\end{aligned} \tag{A1}$$

Using the Pfaff transformation (Eq. (15.3.4) in Ref. [64]) for the hypergeometric function in Eq. (A1), we obtain

$$\begin{aligned}&\frac{4K_\alpha t^\alpha (t+\Delta)^{\alpha-1}}{\alpha\Gamma(\alpha)^2}\times {}_2F_1\left(1-\alpha, 1; 1+\alpha; \frac{t}{t+\Delta}\right) \\ &\quad = \frac{4K_\alpha t^\alpha \Delta^{\alpha-1}}{\alpha\Gamma(\alpha)^2}\times {}_2F_1\left(1-\alpha, \alpha; 1+\alpha; -\frac{t}{\Delta}\right).\end{aligned} \tag{A2}$$

With the relation between the hypergeometric function and the H-function, Eq. (1.131) in Ref. [95] as well as Eq. (8.3.2.7) in Ref. [66], we get

$$ {}_2F_1\left(1-\alpha,\alpha;\alpha+1;-\frac{t}{\Delta}\right)=\frac{\alpha}{\Gamma(1-\alpha)}H^{1,2}_{2,2}\left[\frac{t}{\Delta}\middle|\begin{matrix}(\alpha,1),(1-\alpha,1)\\(0,1),(-\alpha,1)\end{matrix}\right]=\frac{\alpha}{\Gamma(1-\alpha)}H^{2,1}_{2,2}\left[\frac{\Delta}{t}\middle|\begin{matrix}(1,1),(1+\alpha,1)\\(1-\alpha,1),(\alpha,1)\end{matrix}\right]. \tag{A3}$$

This yields an alternative form for the MSI, namely,

$$ \langle x_\Delta^2(t)\rangle=\frac{2K_\alpha t^{2\alpha-1}}{(2\alpha-1)\Gamma(\alpha)^2}\left[\left(1+\frac{\Delta}{t}\right)^{2\alpha-1}+1\right]-\frac{4K_\alpha t^\alpha\Delta^{\alpha-1}}{\Gamma(\alpha)^2\Gamma(1-\alpha)}H^{2,1}_{2,2}\left[\frac{\Delta}{t}\middle|\begin{matrix}(1,1),(1+\alpha,1)\\(1-\alpha,1),(\alpha,1)\end{matrix}\right]. \tag{A4}$$

The first term in Eq. (A4) can be transformed into the series

$$ \begin{aligned}\text{first term}&=\frac{2K_\alpha t^{2\alpha-1}}{(2\alpha-1)\Gamma(\alpha)^2}\left[2+\sum_{k=1}^{+\infty}\binom{2\alpha-1}{k}\left(\frac{\Delta}{t}\right)^k\right]\\&=\frac{2K_\alpha t^{2\alpha-1}}{\Gamma(\alpha)^2}\left[\frac{2}{2\alpha-1}+\frac{\Delta}{t}+(\alpha-1)\left(\frac{\Delta}{t}\right)^2+O\left(\left(\frac{\Delta}{t}\right)^3\right)\right].\end{aligned} \tag{A5}$$

To expand the second term (the H-function) in Eq. (A4), one needs to be more careful since different expansions need to be implemented based on the value of α.

When $\alpha\neq 1,\ 3/2,\ 2,\ 5/2,\ldots$, we are allowed to use expansion (8.2.3.3) in Ref. [66] at $\Delta\ll t$,

$$ H^{2,1}_{2,2}\left[\frac{\Delta}{t}\middle|\begin{matrix}(1,1),(1+\alpha,1)\\(1-\alpha,1),(\alpha,1)\end{matrix}\right]=\sum_{k=0}^{+\infty}\frac{(-1)^k\Gamma(1+k-\alpha)}{(2\alpha-1-k)k!}\left(\frac{\Delta}{t}\right)^{1-\alpha+k}+\sum_{k=0}^{+\infty}\frac{(-1)^k\Gamma(1-k-2\alpha)\Gamma(k+\alpha)}{\Gamma(1-k)k!}\left(\frac{\Delta}{t}\right)^{\alpha+k}. \tag{A6}$$

Since the Gamma function has simple poles at nonpositive integers [96], only the single term $k=0$ survives in the second summation of Eq. (A6). Then the second term in Eq. (A4) can be written as

$$ \begin{aligned}\text{second term}&=\frac{4K_\alpha t^{2\alpha-1}}{\Gamma(\alpha)^2\Gamma(1-\alpha)}\left[\sum_{k=0}^{+\infty}\frac{(-1)^k\Gamma(1+k-\alpha)}{(2\alpha-1-k)k!}\left(\frac{\Delta}{t}\right)^k+\frac{2\Gamma(1-2\alpha)\Gamma(\alpha)}{\Gamma(1-\alpha)}\left(\frac{\Delta}{t}\right)^{2\alpha-1}\right]\\&=\frac{2K_\alpha t^{2\alpha-1}}{\Gamma(\alpha)^2}\left[\frac{2}{2\alpha-1}+\frac{\Delta}{t}+\frac{(2-\alpha)(1-\alpha)}{2\alpha-3}\left(\frac{\Delta}{t}\right)^2+O\left(\left(\frac{\Delta}{t}\right)^3\right)+\frac{2\Gamma(1-2\alpha)\Gamma(\alpha)}{\Gamma(1-\alpha)}\left(\frac{\Delta}{t}\right)^{2\alpha-1}\right].\end{aligned} \tag{A7}$$

Substituting Eqs. (A5) and (A7) into Eq. (A4), one can see that the main order terms proportional to $t^{2\alpha-1}(\Delta/t)^0$ and $t^{2\alpha-1}(\Delta/t)^1$ cancel out. With the main remaining terms we obtain

$$ \langle x_\Delta^2(t)\rangle=\frac{2K_\alpha t^{2\alpha-1}}{\Gamma(\alpha)^2}\left[\frac{(\alpha-1)^2}{2\alpha-3}\left(\frac{\Delta}{t}\right)^2-\frac{2\Gamma(1-2\alpha)\Gamma(\alpha)}{\Gamma(1-\alpha)}\left(\frac{\Delta}{t}\right)^{2\alpha-1}\right]. \tag{A8}$$

When $1/2<\alpha<3/2$, the MSI at long times $t\gg\Delta$ in Eq. (A8) is dominated by the second term; using Euler's reflection formula of the Gamma function, $\Gamma(z)\Gamma(1-z)=\pi/\sin(\pi z)$, for $z\notin\mathbb{Z}$, we arrive at the approximation

$$ \langle x_\Delta^2(t)\rangle\sim-\frac{4K_\alpha\Gamma(1-2\alpha)}{\Gamma(\alpha)\Gamma(1-\alpha)}\Delta^{2\alpha-1}=\frac{2K_\alpha}{\Gamma(2\alpha)|\cos(\pi\alpha)|}\Delta^{2\alpha-1}. \tag{A9}$$

When $\alpha>3/2$, the MSI in Eq. (A8) is dominated by the first term and asymptotically reads

$$ \langle x_\Delta^2(t)\rangle\sim\frac{2K_\alpha(\alpha-1)^2}{(2\alpha-3)\Gamma(\alpha)^2}t^{2\alpha-3}\Delta^2. \tag{A10}$$

We note that for $\alpha=1,\ 3/2,\ 2,\ 5/2,\ldots$ are all the singular points in the series expansion (A6) that need to be excluded. Next, we consider the cases $\alpha=3/2,\ 5/2,\ 7/2,\ldots$, and $\alpha=1,\ 2,\ 3,\ldots$, respectively. In the former situation, the series of the H-function should be more complicated, with power-logarithmic expansions; and in the latter, the H-function expansion fails. In that case we expand the hypergeometric function in Eq. (A1) rather than the H-function in Eq. (A4).

When $\alpha=3/2,\ 5/2,\ 7/2,\ldots,$, using the power-logarithmic expansions (1.4.7) from Ref. [97] in Eq. (A4), we find

$$ H^{2,1}_{2,2}\left[\frac{\Delta}{t}\middle|\begin{matrix}(1,1),(1+\alpha,1)\\(1-\alpha,1),(\alpha,1)\end{matrix}\right]=\sum_{k=0}^{2\alpha-2}\frac{(-1)^k\Gamma(k+1-\alpha)}{(2\alpha-k-1)k!}\left(\frac{\Delta}{t}\right)^{1-\alpha+k}-\frac{\Gamma(\alpha)}{\Gamma(2\alpha)}\left(\frac{\Delta}{t}\right)^\alpha\ln\left(\frac{\Delta}{t}\right)+O\left(\left(\frac{\Delta}{t}\right)^\alpha\ln\left(\frac{\Delta}{t}\right)\right). \tag{A11}$$

Then the second term in the MSI (A4) asymptotically reads for $t \gg \Delta$

$$\text{second term} \sim \frac{4K_\alpha t^{2\alpha-1}}{\Gamma(\alpha)^2\Gamma(1-\alpha)}\left[\sum_{k=0}^{2\alpha-2}\frac{(-1)^k\Gamma(k+1-\alpha)}{(2\alpha-k-1)k!}\left(\frac{\Delta}{t}\right)^k - \frac{\Gamma(\alpha)}{\Gamma(2\alpha)}\left(\frac{\Delta}{t}\right)^{2\alpha-1}\ln\left(\frac{\Delta}{t}\right) + O\left(\left(\frac{\Delta}{t}\right)^{2\alpha-1}\ln\left(\frac{\Delta}{t}\right)\right)\right]. \tag{A12}$$

When $\alpha = 3/2$, this second term is

$$\text{second term} \sim \frac{8K_{3/2}t^2}{\pi}\left[1 + \frac{\Delta}{t} - \frac{1}{4}\left(\frac{\Delta}{t}\right)^2\ln\left(\frac{\Delta}{t}\right) + O\left(\left(\frac{\Delta}{t}\right)^2\ln\left(\frac{\Delta}{t}\right)\right)\right]. \tag{A13}$$

Substituting Eqs. (A13) and (A5) into Eq. (A4), we arrive at the MSI with $\alpha = 3/2$ at long times $t \gg \Delta$,

$$\left\langle x_\Delta^2(t)\right\rangle \sim \frac{2K_{3/2}}{\pi}\Delta^2\ln\left(\frac{t}{\Delta}\right). \tag{A14}$$

When $\alpha \geqslant 5/2$, namely, for $\alpha = 5/2,\ 7/2,\ 9/2, \ldots$, the second term asymptotically reads

$$\begin{aligned}\text{second term} \sim \frac{2K_\alpha t^{2\alpha-1}}{\Gamma(\alpha)^2}\Bigg[&\frac{2}{2\alpha-1} + \frac{\Delta}{t} + \frac{(2-\alpha)(1-\alpha)}{(2\alpha-3)}\left(\frac{\Delta}{t}\right)^2 \\ &+ \frac{2\Gamma(\alpha)}{\Gamma(2\alpha)\Gamma(1-\alpha)}\left(\frac{\Delta}{t}\right)^{2\alpha-1}\ln\left(\frac{\Delta}{t}\right) + O\left(\left(\frac{\Delta}{t}\right)^{2\alpha-1}\ln\left(\frac{\Delta}{t}\right)\right)\Bigg].\end{aligned} \tag{A15}$$

Substituting Eq. (A15) and Eq. (A5) into Eq. (A4), we obtain the MSI with the leading term as

$$\begin{aligned}\left\langle x_\Delta^2(t)\right\rangle &\sim \frac{2K_\alpha(\alpha-1)^2}{(2\alpha-3)\Gamma(\alpha)^2}t^{2\alpha-3}\Delta^2\left[1 - \frac{2(2\alpha-3)\Gamma(\alpha)}{\Gamma(2\alpha)\Gamma(1-\alpha)(\alpha-1)^2}\left(\frac{\Delta}{t}\right)^{2\alpha-3}\ln\left(\frac{\Delta}{t}\right)\right] \\ &\sim \frac{2K_\alpha(\alpha-1)^2}{(2\alpha-3)\Gamma(\alpha)^2}t^{2\alpha-3}\Delta^2.\end{aligned} \tag{A16}$$

This result is identical to Eq. (A10).

When $\alpha = 1,\ 2,\ 3,\ 4, \ldots$, we turn to the hypergeometric function (A2) and then use formulas (15.8.6) and (15.2.4) in Ref. [96] with $\alpha \in \mathbb{N}^+$,

$${}_2F_1\left(1-\alpha, \alpha; 1+\alpha; -\frac{t}{\Delta}\right) = \frac{(\alpha)_{\alpha-1}}{(1+\alpha)_{\alpha-1}}\left(\frac{t}{\Delta}\right)^{\alpha-1}{}_2F_1\left(1-\alpha, 1-2\alpha; 2-2\alpha; -\frac{\Delta}{t}\right) \tag{A17}$$

and

$${}_2F_1\left(1-\alpha, 1-2\alpha; 2-2\alpha; -\frac{\Delta}{t}\right) = \sum_{n=0}^{\alpha-1}\binom{\alpha-1}{n}\frac{(1-2\alpha)_n}{(2-2\alpha)_n}\left(\frac{\Delta}{t}\right)^n, \tag{A18}$$

where $(q)_n$ is the (rising) Pochhammer symbol,

$$(q)_n = \begin{cases}1, & n = 0\\ q(q+1)\cdots(q+n-1), & n > 0\end{cases}. \tag{A19}$$

We then rewrite Eq. (A2) in the form with $t > \Delta$

$$\begin{aligned}\frac{4K_\alpha t^\alpha\Delta^{\alpha-1}}{\alpha\Gamma(\alpha)^2}{}_2F_1\left(1-\alpha, \alpha; 1+\alpha; -\frac{t}{\Delta}\right) &= \frac{4K_\alpha t^{2\alpha-1}}{\Gamma(\alpha)^2}\left[\sum_{n=0}^{\alpha-1}\frac{\binom{\alpha-1}{n}}{2\alpha-1-n}\left(\frac{\Delta}{t}\right)^n\right] \\ &= \frac{2K_\alpha t^{2\alpha-1}}{\Gamma(\alpha)^2}\left[\frac{2}{2\alpha-1} + \frac{\Delta}{t} + \frac{(\alpha-1)(\alpha-2)}{2\alpha-3}\left(\frac{\Delta}{t}\right)^2 + \ldots + \left(\frac{\Delta}{t}\right)^{\alpha-1}\right].\end{aligned} \tag{A20}$$

Substituting Eq. (A20) into the MSI (A1) and considering the expansion of the first term in Eq. (A5), one can easily find that at long times $t \gg \Delta$ the cases $\alpha = 1$ (here only the constant remains in Eq. (A20)) and $\alpha = 2, 3, 4, \ldots$ agree with the asymptotics (A9) and (A10), respectively.

APPENDIX B: TAMSD

According to the definition (10) of the TAMSD, the mean TAMSD of RL-FBM can be derived as

$$\left\langle\overline{\delta^2(\Delta)}\right\rangle = \frac{1}{T-\Delta}\int_0^{T-\Delta}\langle[x(t+\Delta)-x(t)]^2\rangle dt$$
$$= \frac{K_\alpha}{\alpha(2\alpha-1)\Gamma(\alpha)^2}\frac{T^{2\alpha}-\Delta^{2\alpha}}{T-\Delta} + \frac{K_\alpha}{\alpha(2\alpha-1)\Gamma(\alpha)^2}(T-\Delta)^{2\alpha-1} - I_\alpha(\Delta,T), \tag{B1}$$

where

$$I_\alpha(\Delta,T) = \frac{4K_\alpha}{\alpha\Gamma(\alpha)^2}\frac{1}{T-\Delta}\int_0^{T-\Delta}(t+\Delta)^{\alpha-1}t^\alpha \times {}_2F_1\left(1-\alpha,1;1+\alpha;\frac{t}{t+\Delta}\right)dt. \tag{B2}$$

Applying the same transformation from the hypergeometric function to the H-function as in Eqs. (A2) and (A3) and the identities (1.16.4.1) and (8.3.2.1) for the H-function in Ref. [66], we obtain

$$I_\alpha(\Delta,T) = \frac{4K_\alpha}{\Gamma(\alpha)^2\Gamma(1-\alpha)}\frac{\Delta^{2\alpha}}{(T-\Delta)}\int_0^{\frac{T-\Delta}{\Delta}} s^\alpha H^{1,2}_{2,2}\left[s\left|\begin{matrix}(\alpha,1),(1-\alpha,1)\\(0,1),(-\alpha,1)\end{matrix}\right.\right]ds$$
$$= \frac{4K_\alpha}{\Gamma(\alpha)^2\Gamma(1-\alpha)}\frac{\Delta^{2\alpha}}{(T-\Delta)}\frac{(T-\Delta)^{\alpha+1}}{\Delta^{\alpha+1}}H^{1,3}_{3,3}\left[\frac{T-\Delta}{\Delta}\left|\begin{matrix}(-\alpha,1),(\alpha,1),(1-\alpha,1)\\(0,1),(-\alpha,1),(-1-\alpha,1)\end{matrix}\right.\right]$$
$$= \frac{4K_\alpha}{\Gamma(\alpha)^2\Gamma(1-\alpha)}\frac{(T-\Delta)^{\alpha}}{\Delta^{1-\alpha}}H^{1,3}_{3,3}\left[\frac{T-\Delta}{\Delta}\left|\begin{matrix}(-\alpha,1),(\alpha,1),(1-\alpha,1)\\(0,1),(-1-\alpha,1),(-\alpha,1)\end{matrix}\right.\right]. \tag{B3}$$

Moreover, using the identities (8.3.2.6) and (8.3.2.7) in Ref. [66] to reduce to lower orders of the H-function, we find

$$H^{1,3}_{3,3}\left[\frac{T-\Delta}{\Delta}\left|\begin{matrix}(-\alpha,1),(\alpha,1),(1-\alpha,1)\\(0,1),(-1-\alpha,1),(-\alpha,1)\end{matrix}\right.\right] = H^{1,2}_{2,2}\left[\frac{T-\Delta}{\Delta}\left|\begin{matrix}(\alpha,1),(1-\alpha,1)\\(0,1),(-1-\alpha,1)\end{matrix}\right.\right]$$
$$= H^{2,1}_{2,2}\left[\frac{\Delta}{T-\Delta}\left|\begin{matrix}(1,1),(2+\alpha,1)\\(1-\alpha,1),(\alpha,1)\end{matrix}\right.\right], \tag{B4}$$

such that the third term in Eq. (B1) yields as

$$I_\alpha(\Delta,T) = \frac{4K_\alpha}{\Gamma(\alpha)^2\Gamma(1-\alpha)}\frac{(T-\Delta)^{\alpha}}{\Delta^{1-\alpha}}H^{2,1}_{2,2}\left[\frac{\Delta}{T-\Delta}\left|\begin{matrix}(1,1),(2+\alpha,1)\\(1-\alpha,1),(\alpha,1)\end{matrix}\right.\right]. \tag{B5}$$

Therefore the alternative expression for the mean TAMSD can be obtained explicitly,

$$\left\langle\overline{\delta^2(\Delta)}\right\rangle = \frac{K_\alpha}{\alpha(2\alpha-1)\Gamma(\alpha)^2}\frac{T^{2\alpha}-\Delta^{2\alpha}}{T-\Delta} + \frac{K_\alpha}{\alpha(2\alpha-1)\Gamma(\alpha)^2}(T-\Delta)^{2\alpha-1}$$
$$- \frac{4K_\alpha}{\Gamma(\alpha)^2\Gamma(1-\alpha)}\frac{(T-\Delta)^{\alpha}}{\Delta^{1-\alpha}}H^{2,1}_{2,2}\left[\frac{\Delta}{T-\Delta}\left|\begin{matrix}(1,1),(2+\alpha,1)\\(1-\alpha,1),(\alpha,1)\end{matrix}\right.\right]. \tag{B6}$$

To obtain the approximations of the TAMSD at long times $T \gg \Delta$, we consider the first and second terms in Eq. (B6),

$$\text{first term} = \frac{K_\alpha T^{2\alpha-1}}{\alpha(2\alpha-1)\Gamma(\alpha)^2}\left[1-\left(\frac{\Delta}{T}\right)^{2\alpha}\right]\left(1-\frac{\Delta}{T}\right)^{-1}$$
$$= \frac{K_\alpha T^{2\alpha-1}}{\Gamma(\alpha)^2}\left[\frac{1}{\alpha(2\alpha-1)} + \frac{1}{\alpha(2\alpha-1)}\frac{\Delta}{T} + \frac{1}{\alpha(2\alpha-1)}\left(\frac{\Delta}{T}\right)^2 + O\left(\left(\frac{\Delta}{T}\right)^2\right)\right] \tag{B7}$$

and

$$\text{second term} = \frac{K_\alpha}{\alpha(2\alpha-1)\Gamma(\alpha)^2}(T-\Delta)^{2\alpha-1}$$
$$= \frac{K_\alpha T^{2\alpha-1}}{\Gamma(\alpha)^2}\left[\frac{1}{\alpha(2\alpha-1)} - \frac{\Delta}{\alpha T} + \frac{\alpha-1}{\alpha}\left(\frac{\Delta}{T}\right)^2 + O\left(\left(\frac{\Delta}{T}\right)^2\right)\right]. \tag{B8}$$

The approach to tackle the third term in Eq. (B6) is analogous to that for the MSI. When $\alpha \neq 1,\ 3/2,\ 2,\ 5/2, \ldots$, using formula (8.2.3.3) from Ref. [66], we get

$$H^{2,1}_{2,2}\left[\frac{\Delta}{T-\Delta}\middle|\begin{matrix}(1,1),(2+\alpha,1)\\(1-\alpha,1),(\alpha,1)\end{matrix}\right] = \sum_{k=0}^{\infty}\frac{(-1)^k\Gamma(k+1-\alpha)}{(2\alpha-k)(2\alpha-k-1)k!}\left(\frac{\Delta}{T-\Delta}\right)^{1-\alpha+k} + \sum_{k=0}^{\infty}\frac{(-1)^k\Gamma(1-2\alpha-k)\Gamma(\alpha+k)}{\Gamma(2-k)k!}\left(\frac{\Delta}{T-\Delta}\right)^{\alpha+k}. \tag{B9}$$

In Eq. (B9), only two terms remain in the second series. With Eq. (B9) we obtain the third term of Eq. (B6) at long times $T \gg \Delta$,

$$\begin{aligned}I_\alpha(\Delta,T) &= \frac{4K_\alpha T^{2\alpha-1}}{\Gamma(\alpha)^2\Gamma(1-\alpha)}\sum_{k=0}^{\infty}\frac{\Gamma(k+1-\alpha)(-1)^k}{(2\alpha-k)(2\alpha-k-1)k!}\left(\frac{\Delta}{T}\right)^k\left(1-\frac{\Delta}{T}\right)^{2\alpha-1-k}\\
&\quad+\frac{4K_\alpha\Delta^{2\alpha-1}}{\Gamma(\alpha)^2\Gamma(1-\alpha)}\sum_{k=0}^{1}\frac{(-1)^k\Gamma(1-2\alpha-k)\Gamma(\alpha+k)}{\Gamma(2-k)k!}\left(\frac{\Delta}{T-\Delta}\right)^k\\
&\sim\frac{2K_\alpha T^{2\alpha-1}}{\Gamma(\alpha)^2}\left[\frac{1}{\alpha(2\alpha-1)}+\frac{1-\alpha}{\alpha(2\alpha-1)}\frac{\Delta}{T}+\left(\frac{1-\alpha}{\alpha(2\alpha-1)}+\frac{\alpha-2}{2(2\alpha-3)}\right)\left(\frac{\Delta}{T}\right)^2+O\left(\left(\frac{\Delta}{T}\right)^2\right)\right]\\
&\quad+\frac{4K_\alpha\Gamma(1-2\alpha)T^{2\alpha-1}}{\Gamma(\alpha)\Gamma(1-\alpha)}\left[\left(\frac{\Delta}{T}\right)^{2\alpha-1}+\frac{1}{2}\left(\frac{\Delta}{T}\right)^{2\alpha}\right].\end{aligned} \tag{B10}$$

Substituting Eqs. (B7), (B8), and (B10) into Eq. (B6), one can see that the main order terms proportional to $T^{2\alpha-1}(\frac{\Delta}{T})^0$ and $T^{2\alpha-1}(\frac{\Delta}{T})^1$ cancel out. We thus obtain the mean TAMSD of RL-FBM at long times $T \gg \Delta$,

$$\left\langle\overline{\delta^2(\Delta)}\right\rangle \sim \frac{2K_\alpha T^{2\alpha-1}}{\Gamma(2\alpha)|\cos(\pi\alpha)|}\left[\left(\frac{\Delta}{T}\right)^{2\alpha-1}+\frac{1}{2}\left(\frac{\Delta}{T}\right)^{2\alpha}\right]+\frac{(\alpha-1)K_\alpha T^{2\alpha-1}}{(2\alpha-3)\Gamma(\alpha)^2}\left(\frac{\Delta}{T}\right)^2. \tag{B11}$$

Moreover, for $1/2 < \alpha < 3/2$ the mean TMASD is dominated by the first term,

$$\left\langle\overline{\delta^2(\Delta)}\right\rangle \sim \frac{2K_\alpha}{\Gamma(2\alpha)|\cos(\pi\alpha)|}\Delta^{2\alpha-1}, \tag{B12}$$

whereas for $\alpha > 3/2$, the third term is dominant,

$$\left\langle\overline{\delta^2(\Delta)}\right\rangle \sim \frac{(\alpha-1)K_\alpha}{(2\alpha-3)\Gamma(\alpha)^2}\Delta^2 T^{2\alpha-3}. \tag{B13}$$

Conversely, for $\alpha = 3/2,\ 5/2,\ 7/2, \ldots$ the power series expansion (B9) fails in Eq. (B6). Instead, we use the power-logarithmic expansion (1.4.7) in Ref. [97],

$$H^{2,1}_{2,2}\left[\frac{\Delta}{T-\Delta}\middle|\begin{matrix}(1,1),(2+\alpha,1)\\(1-\alpha,1),(\alpha,1)\end{matrix}\right] = \sum_{k=0}^{2\alpha-2}\frac{(-1)^k\Gamma(k+1-\alpha)}{(2\alpha-k)(2\alpha-k-1)k!}\left(\frac{\Delta}{T-\Delta}\right)^{1-\alpha+k} - \frac{\Gamma(\alpha)}{\Gamma(2\alpha)}\left(\frac{\Delta}{T-\Delta}\right)^{\alpha}\ln\left(\frac{\Delta}{T-\Delta}\right) + O\left(\left(\frac{\Delta}{T-\Delta}\right)^{\alpha}\ln\left(\frac{\Delta}{T-\Delta}\right)\right), \tag{B14}$$

and then the third term (B5) in the mean TAMSD (B6) in the long-time limit $T \gg \Delta$ reads

$$I_\alpha(\Delta,T) = \frac{4K_\alpha T^{2\alpha-1}}{\Gamma(\alpha)^2\Gamma(1-\alpha)}\left[\sum_{k=0}^{2\alpha-2}\frac{\Gamma(k+1-\alpha)(-1)^k}{(2\alpha-k)(2\alpha-k-1)k!}\left(\frac{\Delta}{T}\right)^k\left(1-\frac{\Delta}{T}\right)^{2\alpha-1-k} - \frac{\Gamma(\alpha)}{\Gamma(2\alpha)}\left(\frac{\Delta}{T}\right)^{2\alpha-1}\ln\left(\frac{\Delta}{T}\right) + O\left(\left(\frac{\Delta}{T}\right)^{2\alpha-1}\ln\left(\frac{\Delta}{T}\right)\right)\right]. \tag{B15}$$

In particular, when $\alpha = 3/2$,

$$I_{3/2}(\Delta,T) = \frac{8K_{3/2}T^2}{\pi}\left[\frac{1}{3}-\frac{\Delta}{6T}-\frac{1}{6}\left(\frac{\Delta}{T}\right)^2+\frac{1}{4}\left(\frac{\Delta}{T}\right)^2\ln\left(\frac{\Delta}{T}\right)+O\left(\left(\frac{\Delta}{T}\right)^2\ln\left(\frac{\Delta}{T}\right)\right)\right]. \tag{B16}$$

Substituting Eqs. (B16), (B7), and (B8) into Eq. (B6), we obtain the mean TAMSD with the leading term in the long-time limit $T \gg \Delta$,

$$\left\langle \overline{\delta^2(\Delta)} \right\rangle \sim \frac{2K_{3/2}}{\pi} \Delta^2 \ln\left(\frac{T}{\Delta}\right). \tag{B17}$$

When $\alpha = 5/2,\ 7/2,\ 9/2, \ldots$, Eq. (B15) reads

$$\begin{aligned} I_\alpha(\Delta, T) \sim{}& \frac{2K_\alpha T^{2\alpha-1}}{\Gamma(\alpha)^2}\Bigg[\frac{1}{\alpha(2\alpha-1)}\left(1-\frac{\Delta}{T}\right)^{2\alpha-1} + \frac{1}{(2\alpha-1)}\left(\frac{\Delta}{T}\right)\left(1-\frac{\Delta}{T}\right)^{2\alpha-2} + \frac{\alpha-2}{2(2\alpha-3)}\left(\frac{\Delta}{T}\right)^2\left(1-\frac{\Delta}{T}\right)^{2\alpha-3} \\ &- \frac{2\Gamma(\alpha)}{\Gamma(2\alpha)\Gamma(1-\alpha)}\left(\frac{\Delta}{T}\right)^{2\alpha-1}\ln\left(\frac{\Delta}{T}\right) + O\left(\left(\frac{\Delta}{T}\right)^{2\alpha-1}\ln\left(\frac{\Delta}{T}\right)\right)\Bigg] \\ \sim{}& \frac{2K_\alpha T^{2\alpha-1}}{\Gamma(\alpha)^2}\left[\frac{1}{\alpha(2\alpha-1)} + \frac{1-\alpha}{\alpha(2\alpha-1)}\left(\frac{\Delta}{T}\right) + \left(\frac{1-\alpha}{\alpha(2\alpha-1)} + \frac{\alpha-2}{2(2\alpha-3)}\right)\left(\frac{\Delta}{T}\right)^2 + O\left(\left(\frac{\Delta}{T}\right)^3\right)\right] \\ &- \frac{4K_\alpha \Delta^{2\alpha-1}}{\Gamma(\alpha)\Gamma(2\alpha)\Gamma(1-\alpha)}\ln\left(\frac{\Delta}{T}\right). \end{aligned} \tag{B18}$$

Substituting Eqs. (B18), (B7), and (B8) into Eq. (B6), one can see that the main order terms proportional to $T^{2\alpha-1}(\Delta/T)^0$ and $T^{2\alpha-1}(\Delta/T)^1$ cancel out. Thus, we obtain the mean TAMSD of RL-FBM in the long-time limit $T \gg \Delta$ as

$$\left\langle \overline{\delta^2(\Delta)} \right\rangle \sim \frac{2K_\alpha}{\Gamma(\alpha)\Gamma(1-\alpha)}\Delta^{2\alpha-1}\ln\left(\frac{\Delta}{T}\right) + \frac{(\alpha-1)K_\alpha}{(2\alpha-3)\Gamma(\alpha)^2}\Delta^2 T^{2\alpha-3} \sim \frac{(\alpha-1)K_\alpha}{(2\alpha-3)\Gamma(\alpha)^2}\Delta^2 T^{2\alpha-3}. \tag{B19}$$

For $\alpha = 1,\ 2,\ 3, \ldots$ we make the variable transformation $z = t/(t+\Delta)$ in Eq. (B2) and use the integral formula (1. 153.11) for the hypergeometric function in Ref. [66]. As result we have

$$I_\alpha(\Delta, T) = \frac{4K_\alpha}{\alpha(\alpha+1)\Gamma(\alpha)^2} T^{2\alpha-1}\left(1-\frac{\Delta}{T}\right)^\alpha {}_2F_1\left(1-\alpha, 2; \alpha+2; 1-\frac{\Delta}{T}\right). \tag{B20}$$

Again, considering the series expansion of the hypergeometric function (A18) with integer α, we arrive at the third term in the mean TAMSD (B1),

$$I_\alpha(\Delta, T) = \frac{4K_\alpha T^{2\alpha-1}}{\alpha(\alpha+1)\Gamma(\alpha)^2}\sum_{n=0}^{\alpha-1}(-1)^n\binom{\alpha-1}{n}\frac{(2)_n}{(2+\alpha)_n}\left(1-\frac{\Delta}{T}\right)^{\alpha+n}. \tag{B21}$$

In particular, for $\alpha = 1$,

$$I_1(\Delta, T) = 2K_1 T\left(1-\frac{\Delta}{T}\right), \tag{B22}$$

and for $\alpha \geqslant 2$,

$$I_\alpha(\Delta, T) = \frac{4K_\alpha T^{2\alpha-1}}{\alpha(\alpha+1)\Gamma(\alpha)^2}\left[A_0 - A_1\frac{\Delta}{T} + A_2\left(\frac{\Delta}{T}\right)^2 + \cdots + (-1)^{\alpha-1}A_{\alpha-1}\left(\frac{\Delta}{T}\right)^{\alpha-1}\right], \tag{B23}$$

where

$$A_n = \sum_{k=0}^{n}\binom{\alpha}{n-k}\frac{{}_2F_1^{(k)}(1-\alpha, 2; \alpha+2; 1)}{k!}. \tag{B24}$$

These factors can be obtained from the properties of the hypergeometric function and its kth ($k \leqslant \alpha - 1$) order derivative with integer α in the form

$${}_2F_1^{(k)}(1-\alpha, 2; \alpha+2; 1) = \frac{(1-\alpha)_k(2)_k}{(\alpha+2)_k}{}_2F_1(1-\alpha+k, 2+k; \alpha+2+k; 1). \tag{B25}$$

Here,

$${}_2F_1(1-\alpha+k, 2+k; \alpha+2+k; 1) = \frac{(\alpha)_{\alpha-1-k}}{(\alpha+2+k)_{\alpha-1-k}}. \tag{B26}$$

Thus Eq. (B23) reads

$$I_\alpha(\Delta, T) = \frac{2K_\alpha T^{2\alpha-1}}{\Gamma(\alpha)^2}\left[\frac{1}{\alpha(2\alpha-1)} - \frac{\alpha-1}{\alpha(2\alpha-1)}\frac{\Delta}{T} + \left(\frac{1}{2\alpha-1} - \frac{1}{\alpha} + \frac{\alpha-2}{2(2\alpha-3)}\right)\left(\frac{\Delta}{T}\right)^2 + O\left(\left(\frac{\Delta}{T}\right)^2\right)\right]. \tag{B27}$$

Substituting Eqs. (B22) and (B27) into the mean TAMSD (B1), respectively, and considering the expansions of the first and second terms, Eqs. (B7) and (B8), respectively, one can easily find that at long times $t \gg \Delta$ the cases $\alpha = 1$ and $\alpha \geqslant 2$ are in agreement with the asymptotics in Eqs. (B12) and (B13), respectively.

APPENDIX C: SIMULATION APPROACH FOR RL-FBM

Here we provide our numerical approach to discretize the stochastic integral representation given by Eq. (23) to generate the trajectories of RL-FBM $x(t)$ at discrete times $t_n = n \times \delta t$, $n = N_+$, for all admissible values $\alpha > 1/2$. To begin, we discretize the stochastic integral,

$$x(t_n) = \frac{\sqrt{2K_\alpha}}{\Gamma(\alpha)} \sum_{i=0}^{n-1} \int_{t_i}^{t_{i+1}} (t_n - s)^{\alpha-1} \xi(s) ds. \tag{C1}$$

The white Gaussian noise can be approximated by

$$\xi(s) = \nu_i/\sqrt{\delta t}, \tag{C2}$$

where ν_i is a normally distributed random variable with zero mean and unit variance; then we have

$$\begin{aligned} x(t_n) &= \frac{\sqrt{2K_\alpha}}{\Gamma(\alpha)} \sum_{i=0}^{n-1} \left(\frac{\nu_i}{\sqrt{\delta t}}\right) \int_{t_i}^{t_{i+1}} (t_n - s)^{\alpha-1} ds \\ &= \frac{\sqrt{2K_\alpha}}{\Gamma(\alpha)} \sum_{i=0}^{n-1} \left(\frac{\nu_i}{\sqrt{\delta t}}\right) \frac{(t_n - t_i)^\alpha - (t_n - t_i - \delta t)^\alpha}{\alpha} \\ &= \frac{\sqrt{2K_\alpha}}{\Gamma(\alpha)} \sum_{i=0}^{n-1} \left(\frac{\nu_i}{\sqrt{\delta t}}\right) w(t_n - t_i)\delta t, \end{aligned} \tag{C3}$$

with the weight function

$$w(t_n - s) = \frac{(t_n - s)^\alpha - (t_n - s - \delta t)^\alpha}{\alpha \delta t}. \tag{C4}$$

This weight function in Eq. (C4) is the approximation of the kernel $(t_n - s)^{\alpha-1}$ in Eq. (C1) and does not contain any singularity for all $\alpha > 1/2$.

APPENDIX D: AGED ACF OF THE INCREMENTS

The aged ACF of the increments $x^\delta(t) = x(t+\delta) - x(t)$ of RL-FBM is defined as

$$C(t_a, \Delta) = \langle x^\delta(t_a) x^\delta(t_a + \Delta)\rangle, \tag{D1}$$

where δ is a small time step obeying $\delta \ll \Delta$. When $\Delta = 0$, the ACF corresponds to the MSI or aged MSD.

With this notation we obtain

$$\begin{aligned} C(t_a, \Delta) &= \frac{2K_\alpha}{\Gamma(\alpha)^2} \int_0^{t_a+\delta} (t_a + \delta - u)^{\alpha-1} [(t_a + \Delta + \delta - u)^{\alpha-1} - (t_a + \Delta - u)^{\alpha-1}] du \\ &\quad + \frac{2K_\alpha}{\Gamma(\alpha)^2} \int_0^{t_a} (t_a - u)^{\alpha-1} [(t_a + \Delta - u)^{\alpha-1} - (t_a + \Delta + \delta - u)^{\alpha-1}] du. \end{aligned} \tag{D2}$$

After the change of variables $q = t_a + \delta - u$ and $q = t_a - u$ in the first and second integral, respectively, we find

$$\begin{aligned} C(t_a, \Delta) &= \frac{2K_\alpha}{\Gamma(\alpha)^2} \int_0^{t_a} q^{\alpha-1} (q+\Delta)^{\alpha-1} \left[2 - \left(1 + \frac{\delta}{q+\Delta}\right)^{\alpha-1} - \left(1 - \frac{\delta}{q+\Delta}\right)^{\alpha-1}\right] dq \\ &\quad + \frac{2K_\alpha}{\Gamma(\alpha)^2} \int_{t_a}^{t_a+\delta} q^{\alpha-1} (q+\Delta)^{\alpha-1} \left[1 - \left(1 - \frac{\delta}{q+\Delta}\right)^{\alpha-1}\right] dq. \end{aligned} \tag{D3}$$

For a small time step $\delta \to 0$, we consider the series expansion under the condition that $\Delta \gg \delta$ and neglect the higher order terms,

$$\left(1 \pm \frac{\delta}{q+\Delta}\right)^{\alpha-1} \sim 1 \pm (\alpha - 1)\frac{\delta}{q+\Delta} + \frac{(\alpha-1)(\alpha-2)}{2}\left(\frac{\delta}{q+\Delta}\right)^2. \tag{D4}$$

We thus arrive at the ACF

$$\begin{aligned} C(t_a, \Delta) &\sim \frac{2K_\alpha}{\Gamma(\alpha)^2} \left[(\alpha-1)(2-\alpha)\delta^2 \int_0^{t_a} q^{\alpha-1} (q+\Delta)^{\alpha-3} dq + (\alpha - 1)\delta \int_{t_a}^{t_a+\delta} q^{\alpha-1}(q+\Delta)^{\alpha-2} dq\right] \\ &= \frac{2K_\alpha(\alpha-1)}{\Gamma(\alpha)^2} \left\{(2-\alpha)\delta^2 \Delta^{2\alpha-3} \int_0^{\frac{t_a}{\Delta}} q^{\alpha-1}(1+q)^{\alpha-3} dq + \Delta^{2\alpha-2}\delta \int_{\frac{t_a}{\Delta}}^{\frac{t_a+\delta}{\Delta}} q^{\alpha-1}(1+q)^{\alpha-2} dq\right\}. \end{aligned} \tag{D5}$$

Then, for weak aging $t_a \ll \Delta$, we have

$$C(t_a,\Delta) \sim \frac{2K_\alpha(\alpha-1)}{\Gamma(\alpha)^2}\left\{(2-\alpha)\delta^2\Delta^{2\alpha-3}\int_0^{\frac{t_a}{\Delta}} q^{\alpha-1}dq + \Delta^{2\alpha-2}\delta\left[\int_0^{\frac{t_a+\delta}{\Delta}} q^{\alpha-1}dq - \int_0^{\frac{t_a}{\Delta}} q^{\alpha-1}dq\right]\right\}$$
$$= \frac{2K_\alpha(\alpha-1)}{\alpha\Gamma(\alpha)^2}\{(2-\alpha)\delta^2 t_a^\alpha\Delta^{\alpha-3} + \delta\Delta^{\alpha-2}[(t_a+\delta)^\alpha - t_a^\alpha]\}. \quad \text{(D6)}$$

In particular, when $t_a = 0$ the ACF reads

$$C(0,\Delta) \sim \frac{2K_\alpha(\alpha-1)}{\alpha\Gamma(\alpha)^2}\delta^{\alpha+1}\Delta^{\alpha-2}, \quad \text{(D7)}$$

and when $t_a \gg \delta$, we have

$$C(t_a,\Delta) \sim \frac{2K_\alpha(\alpha-1)}{\Gamma(\alpha)^2}\delta^2 t_a^{\alpha-1}\Delta^{\alpha-2}. \quad \text{(D8)}$$

Next we consider the case of strong aging ($t_a \gg \Delta$) for different α.

1. Case $1/2 < \alpha < 3/2$

For $1/2 < \alpha < 3/2$, for strong aging ($t_a \gg \Delta$) we use the following approximation for the first integral in Eq. (D5),

$$\int_0^{\frac{t_a}{\Delta}} q^{\alpha-1}(1+q)^{\alpha-3}dq \approx \int_0^\infty q^{\alpha-1}(1+q)^{\alpha-3}dq = \mathbb{B}(\alpha, 3-2\alpha), \quad \text{(D9)}$$

where the (complete) Beta function is defined by [64]

$$\mathbb{B}(a,b) = \int_0^\infty s^{a-1}(1+s)^{-a-b}ds = \frac{\Gamma(a)\Gamma(b)}{\Gamma(a+b)}. \quad \text{(D10)}$$

The second integral in Eq. (D5) reads

$$\int_{\frac{t_a}{\Delta}}^{\frac{t_a+\delta}{\Delta}} q^{\alpha-1}(1+q)^{\alpha-2}dq \sim \int_{\frac{t_a}{\Delta}}^{\frac{t_a+\delta}{\Delta}} q^{2\alpha-3}dq \sim \left(\frac{\Delta}{t_a}\right)^{3-2\alpha}\frac{\delta}{\Delta}. \quad \text{(D11)}$$

Then, substituting Eqs. (D9) and (D11) into Eq. (D5), we have

$$C(t_a,\Delta) \sim \frac{2K_\alpha(\alpha-1)(2\alpha-1)}{\Gamma(2\alpha)|\cos(\pi\alpha)|}\delta^2\Delta^{2\alpha-3}. \quad \text{(D12)}$$

2. Case $\alpha > 3/2$

For $\alpha > 3/2$ and strong aging ($t_a \gg \Delta$), the first integral in Eq. (D5) diverges as t tends to infinity. We rewrite the first integral in two parts,

$$\int_0^{\frac{t_a}{\Delta}} q^{\alpha-1}(1+q)^{\alpha-3}dq = \int_0^M q^{\alpha-1}(1+q)^{\alpha-3}dq + \int_M^{\frac{t_a}{\Delta}} q^{\alpha-1}(1+q)^{\alpha-3}dq, \quad \text{for } M \gg 1. \quad \text{(D13)}$$

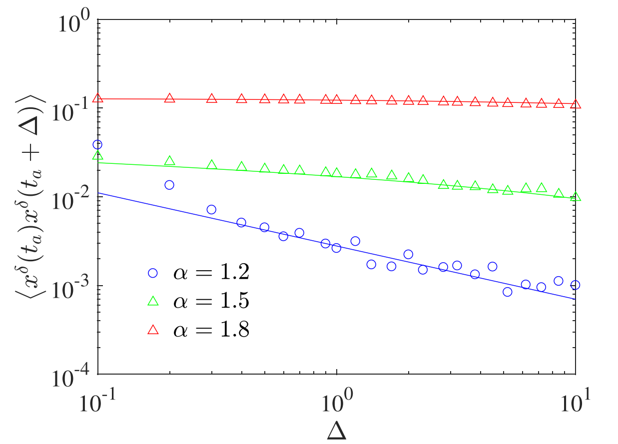

FIG. 5. Simulations (symbols) of the ACF of the increments of RL-FBM at strong aging $t_a \gg \Delta$. The theoretical results (D19) are represented by solid lines. Here we set $t_a = 20$, $\delta = dt = 0.1$, and $K_\alpha = 0.5$.

Then the integral in Eq. (D13) is dominated by the second term and can be approximated as

$$\int_0^{\frac{t_a}{\Delta}} q^{\alpha-1}(1+q)^{\alpha-3}dq \sim \int_M^{\frac{t_a}{\Delta}} q^{\alpha-1}(1+q)^{\alpha-3}dq \sim \int_M^{\frac{t_a}{\Delta}} q^{2\alpha-4}dq \sim \frac{1}{2\alpha-3}\left(\frac{t_a}{\Delta}\right)^{2\alpha-3}. \quad \text{(D14)}$$

The second term in Eq. (D5) can be approximated by Eq. (D11). Then, substituting Eqs. (D14) and (D11) into Eq. (D5), we obtain

$$C(t_a,\Delta) \sim \frac{2K_\alpha(\alpha-1)^2}{(2\alpha-3)\Gamma(\alpha)^2}\delta^2 t_a^{2\alpha-3}. \quad \text{(D15)}$$

3. Case $\alpha = 3/2$

For $\alpha = 3/2$, the first integral in Eq. (D5) can be solved explicitly, and for strong aging $t_a \gg \Delta$, we find an approximation with the leading term

$$\int_0^{t_a/\Delta} q^{1/2}(q+1)^{-3/2}dq = \ln\left(\frac{t_a}{\Delta}\right) + \ln\left(1+\frac{\Delta}{t_a}\right) - 2\sqrt{\frac{t_a}{t_a+\Delta}} \sim \ln\left(\frac{t_a}{\Delta}\right). \quad \text{(D16)}$$

The second term in Eq. (D5) can be approximated by Eq. (D11) with $\alpha = 3/2$,

$$\int_{t_a/\Delta}^{(t_a+\delta)/\Delta} q^{1/2}(1+q)^{-1/2}dq \sim \frac{\delta}{\Delta}. \quad \text{(D17)}$$

Then, substituting Eqs. (D16) and (D17) into Eq. (D5), we get

$$C(t_a,\Delta) \sim \frac{2K_{3/2}}{\pi}\delta^2\ln\left(\frac{t_a}{\Delta}\right). \quad \text{(D18)}$$

To summarize, for strong aging $t_a \gg \Delta$ the ACF of RL-FBM increments for all α is given by

$$C(t_a, \Delta) \sim \begin{cases} \frac{2K_\alpha(\alpha-1)(2\alpha-1)}{\Gamma(2\alpha)|\cos(\pi\alpha)|}\delta^2\Delta^{2\alpha-3}, & 1/2 < \alpha < 3/2 \\ \frac{2K_{3/2}}{\pi}\delta^2 \ln\left(\frac{t_a}{\Delta}\right), & \alpha = 3/2 \\ \frac{2K_\alpha(\alpha-1)^2}{(2\alpha-3)\Gamma(\alpha)^2}\delta^2 t_a^{2\alpha-3}, & \alpha > 3/2. \end{cases} \tag{D19}$$

We note that in the regime $1/2 < \alpha < 3/2$ the ACF becomes stationary and solely depends on the lag time Δ. The consistency of the simulated and analytical ACF for RL-FBM increments at strong aging time $t_a \gg \Delta$ in Eq. (D19) are shown in Fig. 5. A small discrepancy is observed for the case $\alpha = 1.2$ around $\Delta = 0.1$ because the relation $\delta \gg \delta$ is not perfectly fulfilled.

[1] P. Langevin, Sur la théorie du mouvement brownien, C. R. Acad. Sci. (Paris) **146**, 530 (1908).

[2] W. T. Coffey, Y. P. Kalmykov, and J. T. Waldron, *The Langevin Equation: With Applications to Stochastic Problems in Physics, Chemistry and Electrical Engineering* (World Scientific, Singapore, 2004).

[3] R. Zwanzig, *Nonequilibrium Statistical Mechanics* (Oxford University Press, New York, 2001).

[4] N. G. Van Kampen, *Stochastic Processes in Physics and Chemistry* (North Holland, Amsterdam, 1981).

[5] R. Kubo, The fluctuation-dissipation theorem, Rep. Prog. Phys. **29**, 255 (1966).

[6] Y. L. Klimontovich, *Statistical Theory of Open Systems Volume 1: A Unified Approach to Kinetic Description of Processes in Active Systems* (Springer, Berlin, 1995).

[7] R. Klages, G. Radons, and I. M. Sokolov, *Anomalous Transport* (Wiley-VCH Verlag, Berlin, 2008).

[8] A. Pękalski and K. Sznajd-Weron, *Anomalous Diffusion: From Basics to Applications* (Springer, Berlin, 1999).

[9] L. R. Evangelista and E. K. Lenzi, *An Introduction to Anomalous Diffusion and Relaxation* (Springer Nature, Cham, CH, 2023).

[10] M. M. Meerschaert and A. Sikorskii, *Stochastic Models for Fractional Calculus* (Walter de Gruyter GmbH, Berlin, 2019).

[11] J. P. Bouchaud and A. Georges, Anomalous diffusion in disordered media: Statistical mechanisms, models and physical applications, Phys. Rep. **195**, 127 (1990).

[12] R. Metzler and J. Klafter, The random walk's guide to anomalous diffusion: A fractional dynamics approach, Phys. Rep. **339**, 1 (2000).

[13] I. M. Sokolov, Models of anomalous diffusion in crowded environments, Soft Matter **8**, 9043 (2012).

[14] F. Höfling and T. Franosch, Anomalous transport in the crowded world of biological cells, Rep. Prog. Phys. **76**, 046602 (2013).

[15] R. Metzler, J.-H. Jeon, A. G. Cherstvy, and E. Barkai, Anomalous diffusion models and their properties: Nonstationarity, nonergodicity, and ageing at the centenary of single particle tracking, Phys. Chem. Chem. Phys. **16**, 24128 (2014).

[16] A. N. Kolmogorov, Wienersche Spiralen und einige andere interessante Kurven im Hilbertschen Raum, C. R. (Doklady) Acad. Sci. URSS (N. S.) **26**, 115 (1940).

[17] B. B. Mandelbrot and J. W. Van Ness, Fractional Brownian motions, fractional noises and applications, SIAM Rev. **10**, 422 (1968).

[18] H. Qian, *Fractional Brownian Motion and Fractional Gaussian Noise, Processes with Long-Range Correlations: Theory and Applications, Lecture Notes in Physics Vol. 621* (Springer-Verlag, Berlin, 2003).

[19] S. C. Weber, A. J. Spakowitz, and J. A. Theriot, Bacterial chromosomal loci move subdiffusively through a viscoelastic cytoplasm, Phys. Rev. Lett. **104**, 238102 (2010).

[20] J.-H. Jeon, V. Tejedor, S. Burov, E. Barkai, C. Selhuber-Unkel, K. Berg-Sørensen, L. Oddershede, and R. Metzler, In vivo anomalous diffusion and weak ergodicity breaking of lipid granules, Phys. Rev. Lett. **106**, 048103 (2011).

[21] M. Weiss, Single-particle tracking data reveal anticorrelated fractional Brownian motion in crowded fluids, Phys. Rev. E **88**, 010101(R) (2013).

[22] J. Szymanski and M. Weiss, Elucidating the origin of anomalous diffusion in crowded fluids, Phys. Rev. Lett. **103**, 038102 (2009).

[23] O. Vilk, E. Aghion, T. Avgar, C. Beta, O. Nagel, A. Sabri, R. Sarfati, D. K. Schwartz, M. Weiss, D. Krapf, R. Nathan, R. Metzler, and M. Assaf, Unravelling the origins of anomalous diffusion: From molecules to migrating storks, Phys. Rev. Res. **4**, 033055 (2022).

[24] S. Janušonis, J. H. Haiman, R. Metzler, and T. Vojta, Predicting the distribution of serotonergic axons: A supercomputing simulation of reflected fractional Brownian motion in a 3D-mouse brain model, Front. Comput. Neurosci. **17**, 1189853 (2023).

[25] S. Janušonis, N. Detering, R. Metzler, and T. Vojta, Serotonergic axons as fractional brownian motion paths: Insights into the self-organization of regional densities, Front. Comput. Neurosci. **14**, 56 (2020).

[26] F. Comte and E. Renault, Long memory in continuous-time stochastic volatility models, Math. Finance **8**, 291 (1998).

[27] D. Marinucci and P. M. Robinson, Alternative forms of fractional Brownian motion, J. Stat. Plann. Inference **80**, 111 (1999).

[28] J. Gatheral, T. Jaisson, and M. Rosenbaum, Volatility is rough, Quant. Finance **18**, 933 (2018).

[29] H. Mori, Transport, collective motion, and Brownian motion, Prog. Theor. Phys. **33**, 423 (1965).

[30] D. Panja, Generalized Langevin equation formulation for anomalous polymer dynamics, J. Stat. Mech. (2010) L02001.

[31] S. C. Kou, Stochastic modeling in nanoscale biophysics: Subdiffusion within proteins, Ann. Appl. Stat. **2**, 501 (2008).

[32] E. Lutz, Fractional Langevin equation, Phys. Rev. E **64**, 051106 (2001).

[33] W. H. Deng and E. Barkai, Ergodic properties of fractional Brownian-Langevin motion, Phys. Rev. E **79**, 011112 (2009).

[34] D. Molina-Garcia, T. Sandev, H. Pagnini, A. Chechkin, and R. Metzler, Crossover from anomalous to normal diffusion: Truncated power-law noise correlations and applications to dynamics in lipid bilayers, New J. Phys. **20**, 103027 (2008).

[35] M. Caputo, Linear models of dissipation whose Q is almost frequency independent, Ann. Geophys. **19**, 383 (1966).

[36] M. Caputo, Linear models of dissipation whose Q is almost frequency independent-II, Geophys. J. Int. **13**, 529 (1967).

[37] I. Podlubny, *Fractional Differential Equations, Mathematics in Science and Engineering* (Academic Press, New York, 1999).

[38] I. M. Gel'fand and G. E. Shilov, *Generalized Functions, Vol. 1* (Academic Press, New York, 1964).

[39] C. H. Eab and S. C. Lim, Fractional Langevin equations of distributed order, Phys. Rev. E **83**, 031136 (2011).

[40] P. Lévy, *In Random Functions: General Theory with Special Reference to Laplacian Random Functions* (University of California Press, Berkeley, 1953).

[41] S. C. Lim, Fractional Brownian motion and multifractional Brownian motion of Riemann-Liouville type, J. Phys. A: Math. Theor. **34**, 1301 (2001).

[42] Y. Mardoukhi, A. V. Chechkin, and R. Metzler, Spurious ergodicity breaking in normal and fractional Ornstein-Uhlenbeck process, New J. Phys. **22**, 073012 (2020).

[43] I. I. Gikhman and A. V. Skorokhod, *Introduction to the Theory of Random Processes* (W. B. Saunders, Washington, 1969).

[44] A. N. Kolmogorov, The local structure of turbulence in incompressible viscous fluid for very large Reynolds numbers, Dokl. Akad. Nauk. SSSR **30**, 301 (1941).

[45] A. N. Kolmogorov, Dissipation of energy in locally isotropic turbulence, Dokl. Akad. Nauk. SSSR **32**, 19 (1941).

[46] A. M. Yaglom and M. S. Pinsker, Random process with stationary increments of order n, Dokl. Akad. Nauk. SSSR **90**, 731 (1953).

[47] A. M. Yaglom, Correlation theory of processes with random stationary nth increments, Mat. Sb. **37**, 141 (1955).

[48] A. M. Yaglom, *Correlation Theory of Stationary and Related Random Functions, Vol. 1, Basic Results, Vol. 2*, Supplementary Notes and References (Springer, New York, 1987).

[49] E. Barkai, Y. Garini, and R. Metzler, Strange kinetics of single molecules in living cells, Phys. Today **65(8)**, 29 (2012).

[50] C. Manzo and M. F. Garcia-Parajo, A review of progress in single particle tracking: From methods to biophysical insights, Rep. Prog. Phys. **78**, 124601 (2015).

[51] R. Nathan *et al.*, Big-data approaches lead to an increased understanding of the ecology of animal movement, Science **375**, eabg1780 (2022).

[52] O. Vilk, R. Metzler, and M. Assaf, nonMarkovian gene expression, Phys. Rev. Res. **6**, L022026 (2024).

[53] Y. He, S. Burov, R. Metzler, and E. Barkai, Random time-scale invariant diffusion and transport coefficients, Phys. Rev. Lett. **101**, 058101 (2008).

[54] Y. Meroz, I. M. Sokolov, and J. Klafter, Test for determining a subdiffusive model in ergodic systems from single trajectories, Phys. Rev. Lett. **110**, 090601 (2013).

[55] M. Magdziarz, A. Weron, K. Burnecki, and J. Klafter, Fractional Brownian motion versus the continuous-time random walk: A simple test for subdiffusive dynamics, Phys. Rev. Lett. **103**, 180602 (2009).

[56] A. Lubelski, I. M. Sokolov, and J. Klafter, Nonergodicity mimics inhomogeneity in single particle tracking, Phys. Rev. Lett. **100**, 250602 (2008).

[57] J. P. Bouchaud, Weak ergodicity breaking and aging in disordered systems, J. Phys. I France **2**, 1705 (1992).

[58] A. Godec and R. Metzler, Finite-time effects and ultraweak ergodicity breaking in superdiffusive dynamics, Phys. Rev. Lett. **110**, 020603 (2013).

[59] E.-J. Donth, *The Glass Transition* (Springer, Berlin, 2001).

[60] J. H. P. Schulz, E. Barkai, and R. Metzler, Aging effects and population splitting in single-particle trajectory averages, Phys. Rev. Lett. **110**, 020602 (2013).

[61] J. H. P. Schulz, E. Barkai, and R. Metzler, Aging renewal theory and application to random walks, Phys. Rev. X **4**, 011028 (2014).

[62] M. Schwarzl, A. Godec, and R. Metzler, Quantifying nonergodicity of anomalous diffusion with higher order moments, Sci. Rep. **7**, 3878 (2017).

[63] W. Wang, A. G. Cherstvy, A. V. Chechkin, S. Thapa, F. Seno, X. B. Liu, and R. Metzler, Fractional Brownian motion with random diffusivity: Emerging residual nonergodicity below the correlation time, J. Phys. A: Math. Theor. **53**, 474001 (2020).

[64] M. Abramowitz and I. A. Stegun, *Handbook of Mathematical Functions with Formulas, Graphs, and Mathematical Tables* (Dover, New York, 1969).

[65] Q. Wei, W. Wang, H. W. Zhou, R. Metzler, and A. Chechkin, Time-fractional Caputo derivative versus other integrodifferential operators in generalized Fokker-Planck and generalized Langevin equations, Phys. Rev. E **108**, 024125 (2023).

[66] A. Prudnikov, Y. A. Brychkov, and O. Marichev, *Integrals and Series. Volume 3: More Special Functions* (Gordon and Breach, New York, 1990).

[67] M. Balcerek, K. Burnecki, S. Thapa, A. Wyłomańska, and A. V. Chechkin, Fractional Brownian motion with random Hurst exponent: Accelerating diffusion and persistence transitions, Chaos **32**, 093114 (2022).

[68] J. H. P. Schulz, A. V. Chechkin, and R. Metzler, Correlated continuous time random walks: Combining scale-invariance with long-range memory for spatial and temporal dynamics, J. Phys. A: Math. Theor. **46**, 475001 (2013).

[69] A. V. Weigel, B. Simon, M. M. Tamkun, and D. Krapf, Ergodic and nonergodic processes coexist in the plasma membrane as observed by single-molecule tracking, Proc. Natl. Acad. Sci. USA **108**, 6438 (2011).

[70] G. Sikora, K. Burnecki, and A. Wyłomańska, Mean-squared-displacement statistical test for fractional Brownian motion, Phys. Rev. E **95**, 032110 (2017).

[71] H. Seckler, J. Szwabiński, and R. Metzler, Machine-learning solutions for the analysis of single-particle diffusion trajectories, J. Phys. Chem. Lett. **14**, 7910 (2023).

[72] C. Manzo, Extreme learning machine for the characterization of anomalous diffusion from single trajectories (AnDi-ELM), J. Phys. A: Math. Theor. **54**, 334002 (2021).

[73] H. Seckler and R. Metzler, Bayesian deep learning for error estimation in the analysis of anomalous diffusion, Nat. Commun. **13**, 6717 (2022).

[74] P. Kowalek, H. Loch-Olszewska, and J. Szwabiński, Classification of diffusion modes in single-particle tracking data: Feature-based versus deep-learning approach, Phys. Rev. E **100**, 032410 (2019).

[75] H. Seckler and R. Metzler, Change-point detection in anomalous-diffusion trajectories utilising machine-learning-based uncertainty estimates, J. Phys. Phot. **6**, 045025 (2024).

[76] G. Muñoz-Gil *et al.*, Objective comparison of methods to decode anomalous diffusion, Nat. Commun. **12**, 6253 (2021).

[77] N. Granik, L. E. Weiss, E. Nehme, M. Levin, M. Chein, E. Perlson, Y. Roichman, and Y. Shechtman, Single-particle diffusion characterization by deep learning, Biophys. J. **117**, 185 (2019).

[78] S. Thapa, M. A. Lomholt, J. Krog, A. G. Cherstvy, and R. Metzler, Bayesian analysis of single-particle tracking data using the nested-sampling algorithm: Maximum-likelihood model selection applied to stochastic-diffusivity data, Phys. Chem. Chem. Phys. **20**, 29018 (2018).

[79] A. Robson, K. Burrage, and M. C. Leake, Inferring diffusion in single live cells at the single-molecule level, Philos. Trans. R. Soc. B **368**, 20120029 (2013).

[80] A. Sabri, X. Xu, D. Krapf, and M. Weiss, Elucidating the origin of heterogeneous anomalous diffusion in the cytoplasm of mammalian cells, Phys. Rev. Lett. **125**, 058101 (2020).

[81] K. Norregaard, R. Metzler, C. Ritter, K. Berg-Sørensen, and L. Oddershede, Manipulation and motion of organelles and single molecules in living cells, Chem. Rev. **117**, 4342 (2017).

[82] N. Korabel, D. Han, A. Taloni, G. Pagnini, S. Fedotov, V. Allan, and T. A. Waigh, Unravelling heterogeneous transport of endosomes, E-print arXiv:2107.07760.

[83] D. Han, N. Korabel, R. Chen, M. Johnston, A. Gavrilova, V. J. Allan, S. Fedotov, and T. A. Waigh, Deciphering anomalous heterogeneous intracellular transport with neural networks, ELife **9**, e52224 (2020).

[84] V. M. Worlitzer, A. Jose, I. Grinberg, M. Bär, S. Heidenreich, A. Eldar, G. Ariel, and A. Be'er, Biophysical aspects underlying the swarm to biofilm transition, Sci. Adv. **8**, eabn8152 (2022).

[85] H. A. Shaban, R. Barth, L. Recoules, and K. Bystricky, Hi-D: Nanoscale mapping of nuclear dynamics in single living cells, Genome Biol. **21**, 95 (2020).

[86] N. Korabel, G. D. Clemente, D. Han, F. Feldman, T. H. Millard, and T. A. Waigh, Hemocytes in Drosophila melanogaster embryos move via heterogeneous anomalous diffusion, Commun. Phys. **5**, 269 (2022).

[87] T. A. Waigh and N. Korabel, Heterogeneous anomalous transport in cellular and molecular biology, Rep. Prog. Phys. **86**, 126601 (2023).

[88] W. Wang, M. Balcerek, K. Burnecki, A. V. Chechkin, S. Janušonis, J. Ślęzak, T. Vojta, A. Wyłomańska, and R. Metzler, Memory-multi-fractional Brownian motion with continuous correlations, Phys. Rev. Res. **5**, L032025 (2023).

[89] J. Ślęzak and R. Metzler, Minimal model of diffusion with time changing Hurst exponent, J. Phys. A: Math. Theor. **56**, 35LT01 (2023).

[90] M. Balcerek, A. Wyłomańska, K. Burnecki, R. Metzler, and D. Krapf, Modelling intermittent anomalous diffusion with switching fractional Brownian motion, New J. Phys. **25**, 103031 (2023).

[91] K. Hasselmann, Stochastic climate models Part I. Theory, Tellus **28**, 473 (1976).

[92] N. W. Watkins, R. Calel, S. C. Chapman, A. Chechkin, R. Klages, and D. A. Stainforth, The challenge of non-Markovian energy balance models in climate, Chaos **34**, 072105 (2024).

[93] O. Tal-Friedman, A. Pal, A. Sekhon, S. Reuveni, and Y. Roichman, Experimental realization of diffusion with stochastic resetting, J. Phys. Chem. Lett. **11**, 7350 (2020).

[94] L. Giuggioli, T. J. McKetterick, V. M. Kenkre, and M. Chase, Fokker-Planck description for a linear delayed Langevin equation with additive Gaussian noise, J. Phys. A: Math. Theor. **49**, 384002 (2016).

[95] A. M. Mathai, R. K. Saxena, and H. J. Haubold, *The H-Function, Theory and Applications* (Springer, New York, 2010).

[96] F. W. Olver, D. W. Lozier, R. F. Boisvert, and C. W. Clark, *NIST Handbook of Mathematical Functions* (Cambridge University Press, New York, 2010).

[97] A. A. Kilbas and M. Saigo, *H-Transforms: Theory and Applications* (CRC Press, Boca Raton, 2004).